TR 88-002

EIDETICS
INTERNATIONAL
VISUAL AERODYNAMICS DIVISION

February 1988

AN INNOVATIVE APPROACH TO NONINTRUSIVE QUANTITATIVE MEASUREMENTS OF VORTEX FLOWS

GERALD N. MALCOLM
LIANE C. LEWIS
BERT F. AYERS
DANIEL M. GOLDFARB

EIDETICS INTERNATIONAL, INC.
VISUAL AERODYNAMICS DIVISION

AND

DONALD T. WARD
STEVEN L. MORRIS

AEROSPACE ENGINEERING DEPARTMENT
TEXAS A&M UNIVERSITY

Prepared for:

USAF Contract No. F49620-87-C-0069
Directorate of Aerospace Sciences
AFOSR
Bolling AFB, DC 20332-6448

"Original contains color plates: All DTIC reproductions will be in black and white"

UNCLASSIFIED

SECURITY CLASSIFICATION OF THIS PAGE

REPORT DOCUMENTATION PAGE

1a. REPORT SECURITY CLASSIFICATION UNCLASSIFIED	1b RESTRICTIVE MARKINGS
2a. SECURITY CLASSIFICATION AUTHORITY	3 DISTRIBUTION / AVAILABILITY OF REPORT APPROVED FOR PUBLIC RELEASE DISTRIBUTION IS UNLIMITED
2b. DECLASSIFICATION / DOWNGRADING SCHEDULE	
4. PERFORMING ORGANIZATION REPORT NUMBER(S)	5 MONITORING ORGANIZATION REPORT NUMBER(S) AFOSR-TR- 88-0403
6a. NAME OF PERFORMING ORGANIZATION EIDETICS INT 6b OFFICE SYMBOL (If applicable)	7a NAME OF MONITORING ORGANIZATION AFOSR/NA
6c. ADDRESS (City, State, and ZIP Code) 3669 W. 240th ST TORRANCE CA 90505	7b ADDRESS (City, State, and ZIP Code) BUILDING 410 BOLLING AFB, DC 20332-6448
8a. NAME OF FUNDING / SPONSORING ORGANIZATION AFOSR 8b OFFICE SYMBOL (If applicable) NA	9 PROCUREMENT INSTRUMENT IDENTIFICATION NUMBER F49620-87-C-0069
8c. ADDRESS (City, State, and ZIP Code) BUILDING 410 BOLLING AFB, DC 20332-6448	10 SOURCE OF FUNDING NUMBERS PROGRAM ELEMENT NO: 61102F PROJECT NO: 2307 TASK NO: A3 WORK UNIT ACCESSION NO:
11 TITLE (Include Security Classification) (U) An Innovative Approach to Nonintrusive Quantitative Measurements of Vortex Flows	
12 PERSONAL AUTHOR(S) Malcolm, Lewis, Ayers, Goldfarb	
13a. TYPE OF REPORT Final	13b TIME COVERED FROM 01/87 TO 12/87
14 DATE OF REPORT (Year, Month, Day) 02/88	15 PAGE COUNT 45
16. SUPPLEMENTARY NOTATION	

17 COSATI CODES		
FIELD	GROUP	SUB-GROUP

18 SUBJECT TERMS (Continue on reverse if necessary and identify by block number)
Flow Visualization, Flow Measurement, Vortex Flows.

19 ABSTRACT (Continue on reverse if necessary and identify by block number)

A unique flow measurement technique was used to obtain quantitative vortex flow field data. This demonstration demonstrated that a video based data acquisition system, "Expertvision", could be used to measure the velocity of flow through some parts of the flow field. The system systematically tracks packets of colored dye emjected from the models into there surrounding flow fields and then subsequently reduces the data to position, velocity and acceleration measurements for individual vortex cores. Vortex core data were collected for 70 and 80 degree delta wing models with both stationary and forced roll oscillation roll conditions.

20. DISTRIBUTION / AVAILABILITY OF ABSTRACT ☐ UNCLASSIFIED/UNLIMITED ☒ SAME AS RPT	21 ABSTRACT SECURITY CLASSIFICATION UNCLASSIFIED
22a. NAME OF RESPONSIBLE INDIVIDUAL HENRY E. HELIN, CAPTAIN, USAF	22b TELEPHONE (Include Area Code) 202-767-0471 22c OFFICE SYMBOL AFOSR/NA

DD FORM 1473, 84 MAR 83 APR edition may be used until exhausted
All other editions are obsolete

SECURITY CLASSIFICATION OF THIS PAGE
UNCLASSIFIED

TR 88-002

EIDETICS
INTERNATIONAL

VISUAL AERODYNAMICS DIVISION

February 1988

AN INNOVATIVE APPROACH TO NONINTRUSIVE QUANTITATIVE MEASUREMENTS OF VORTEX FLOWS

GERALD N. MALCOLM

LIANE C. LEWIS

BERT F. AYERS

DANIEL M. GOLDFARB

AND

DONALD T. WARD

STEVEN L. MORRIS

AEROSPACE ENGINEERING DEPARTMENT
TEXAS A&M UNIVERSITY

Prepared for:

USAF Contract No. F49620-87-C-0069
Directorate of Aerospace Sciences
AFOSR
Bolling AFB, DC 20332-6448

APPENDIX B
DOD No. 88.1

U.S. DEPARTMENT OF DEFENSE

SMALL BUSINESS INNOVATION RESEARCH (SBIR) PROGRAM
PHASE I -FY 1988
PROJECT SUMMARY

Topic No. AF87-241 Military Department/Agency USAF

Name and Address of Proposing Small Business Firm

Eidetics International, Inc. - Visual Aerodynamics Division
3669 W. 240th Street
Torrance, CA 90505

Name and Title of Principal Investigator

Gerald N. Malcolm, Vice-President, Visual Aerodynamics Division

Proposal Title

"An Innovative Approach to Nonintrusive Quantitative Measurements of Vortex Flows"

Technical Abstract (Limit your abstract to 200 words with no classified or proprietary information/data)

The flow fields around modern aircraft configurations are typically dominated by complex three-dimensional vortex flows. Flow visualization techniques are effective in both wind and water tunnels to increase the understanding of vortex flow fields. A unique non-intrusive flow measurement technique was used to explore a novel method of obtaining quantitative vortex flow field data. This investigation demonstrated that a video-based data acquisition system, ExpertVision™, could be used to measure the velocity of flow through some parts of the flow field. The system systematically tracks pulses or "packets" of colored dye ejected from the models into their surrounding flow fields and then subsequently reduces the data to position, velocity, and acceleration measurements for individual vortex cores. Vortex core data were collected from 70° and 80° delta wing models with both stationary and forced roll oscillation conditions. ExpertVision was used "off-line" to reduce and analyze trajectory, velocity, and acceleration profiles of dye pulses injected in two planes (planform and side views). The static data indicate all trends to be consistent, although absolute magnitudes of vortex burst point locations were consistently 10%-15% further forward than other experimental measurements indicate. The velocity data matched other measurements and theory reasonably well. The forced oscillation measurements were unique so far as is known by the authors in providing measured phase correlations between model motion and vortex movement as well as phasing between model motion and vortex burst point movement. It is strongly recommended that this video-imaging scheme be further developed and, specifically, that three-dimensional capability be added to the system.

Anticipated Benefits/Potential Commercial Applications of the Research or Development

Development of this nonintrusive flow measurement system can lead to a number of benefits and applications. The capability for nonintrusive flow measurements provides the potential for acquiring detailed knowledge of unsteady vortex flow characteristics of delta wings and fighter models. The experimental technique can be a valuable measurement tool for research in fluid flows and could be made available to the entire research community. In addition to providing the means for nonintrusive flow measurements to present and future water tunnel users, Eidetics would be able to offer this capability as an in-house measurement capability to support DOD research and development contracts and for outside commercial airframe companies using the Eidetics water tunnel.

List a maximum of 8 Key Words that describe the Project.

Water tunnel flow visualization
Nonintrusive flow measurements
Vortex flows

Nothing on this page is classified or proprietary information/data

TABLE OF CONTENTS

"Original copy [illegible] pages. All DTIC reproductions will be in black and white"

LIST OF TABLES AND FIGURES

1.0 INTRODUCTION

The aerodynamic characteristics of modern fighter aircraft are influenced significantly by the nature and complexity of their vortex-dominated flow fields. The use of vortex lift on wings and wing leading edge extensions has provided needed enhancements to the maneuverability of newer fighter configurations. Considerable interest and research efforts have been generated to exploit means of controlling these vortices to improve stability and controllability. Several techniques have been utilized in both water and wind tunnels to visualize these flow fields. Figure 1, for example, shows an example of the complex vortex flow field of a generic fighter model as visualized in a water tunnel. Vortices from the forebody, wing, and wing leading edge extension (LEX) can be seen clearly. Several techniques have been developed to obtain quantitative as well as qualitative information for these flow fields. Nonintrusive methods such as laser velocimeters (LV) and intrusive methods such as hot wire anemometer probes, vortometers, and pitot tubes have all been used with varying degrees of success. The disadvantage of intrusive methods is that the probes can significantly alter the flow field, particularly in a vortex where the burst location can be very sensitive to even minor pressure gradients introduced by a probe. The laser velocimeter technique is very good for detailed measurements of all parts of the flow field, but it is quite expensive to purchase and operate and requires thoroughly trained personnel to set up and operate effectively. The need exists for a reasonably simple quantitative measuring system that fits in the utility area between a complex LV system and typical flow visualization methods. It would be particularly advantageous if the method could provide quantitative measurements simultaneously with detailed flow visualization such as that obtained in water tunnels. It needs to be relatively easy to learn to use and, most importantly, be compatible with recorded video images, since this medium is most often used for flow visualization documentation. This approach also allows the data analysis to be completed after the test. However, careful attention must still be paid to proper experimental setup to insure that the video images to be processed later will have the quality necessary for the data processing system to be effective.

2.0 OBJECTIVES AND APPROACH

The primary purpose of this study was to determine if a newly-developed video digital imaging system, ExpertVision™, could be utilized to perform nonintrusive quantitative measurements of vortex flows on simple aircraft-like models in a water tunnel. While the primary goal was to demonstrate the ability to make quantitative measurements, it was also hoped that more could be learned about the fluid mechanics of delta wings at moderate to high angles of attack even while developing the measurement tool.

The approach was to conduct experiments on two delta-wing models in the Eidetics International Flow Visualization Water Tunnel (Figure 2) and evaluate the capability of ExpertVision to determine specific flow parameters. The parameters that were measured were (1) the leading edge vortex core positions and angles with respect to the model surface, (2) the location of the vortex burst points, and (3)

the velocity of the fluid in the vortex core from its origin at the wing apex to the point where the vortex bursts.

Experiments were conducted initially with 70° and 80° delta wing models held stationary at various pitch and yaw angles, α_T and β_T.* Later, experiments were conducted with models mounted on a forced oscillation in roll apparatus. For the static experiments, the angle of attack (or pitch) ranged from 10° to 40° with sideslip (or yaw) angles up to 10°. For the forced oscillation experiments, the angle of attack ranged from 15° to 35° with amplitude of roll oscillations up to ±30° and reduced frequencies, $\omega b/2V$, up to 1.0.

3.0 TEST TECHNIQUE

The basic instrumentation system used for flow field measurements was a video-based computer system that systematically tracked moving images recorded on video tape. ExpertVision equipment can track and analyze any image, such as a point or "target" on a body surface, that can be isolated to provide edge detection of the image in the video processor. Initial work was aimed at optimizing the colors and contrasts of the dye, models, and background, and also to determine the best method for pulsing the dye source. Rather than using continuous dye flow, as is typical for flow visualization in a water tunnel (Figure 1), the injected dye was pulsed to produce small "packets" of dye which served as targets as they travelled through the flow field. It was quickly shown that dye packets were feasible targets for tracking ExpertVision. Experiments were initially conducted with a NACA 2412 airfoil to attempt to gather flow velocity data over a two-dimensional model to correlate with calculated theoretical data. However, to provide a sufficient chordwise length of travel for the dye packets to be analyzed by ExpertVision, the aspect ratio was too low to adequately simulate two-dimensional flow. In addition, since Reynolds number was low (?5,000 based on a cord of 10 inches), the flow was laminar and separated very easily. After separation, the dye diffused rapidly and could not be tracked. The two-dimensional airfoil experiment was subsequently dropped. However, both 70° and 80° delta wing models were tested. Tests were performed initially with the models held stationary at a desired α_T and β_T, then later oscillated at pre-determined roll rates at an amplitude of ±30° for selected angles of attack.

At mid to high angles of attack, these delta wings produce a well-defined vortex from each leading edge, which were easily traceable by ExpertVision. Only flow directly in the vortex core was investigated, as following dye in the outer structure of a vortex proved to be too difficult. Figures 3 and 4 show examples of the vortex flows observed on the delta-wing models. Figure 3 shows a continuous dye flow. Figure 4 shows an example of the "pulsed" dye flow. The forced roll oscillation

* These pitch and yaw angles, α_T and β_T, are approximately the same as body axis angle of attack and sideslip, α and β. That is, $\tan \alpha = \tan \alpha_T / \cos \beta_T$ and $\sin \beta = \cos \alpha_T \sin \beta_T$.

investigations were conducted to determine the response of a flow field to the motion of a model. A photograph of a model mounted on the forced oscillation rig in the water tunnel is shown in Figure 5. The model and vortex core motion were simultaneously tracked by the ExpertVision system by following the pulsed dye packets in the flow and the movement of reference points located on the surface of the model.

The experiments were jointly conducted by Eidetics International and the Aerospace Engineering Department at Texas A&M University. Eidetics' primary responsibilities included the design and construction of the models and support systems, conducting the water tunnel tests and optimizing the visual image, and participating in the analysis of the reduced video data. The ExpertVision system was provided by Texas A&M University. Their responsibility was to consult on the data gathering effort and to lead the effort to analyze the video data on ExpertVision at reduction facilities located at Texas A&M. Eidetics and Texas A&M collaborated on the evaluation of the results.

4.0 TEST FACILITIES AND CONDITIONS

Two sets of experiments were conducted in the Eidetics International Visual Aerodynamics Division 1520 Flow Visualization Water Tunnel. The facility is a continuous horizontal flow tunnel with a test section 20" high x 15" wide x 60" long (Figures 2 and 6). The test section is a channel constructed of tempered glass which allows both side and planform views. In addition, a downstream transverse window provides an upstream end view without any flow obstruction. Although the tunnel speed can be varied from 0 to 1 ft/sec, for most of this test the flow rate was set at 0.33 ft/sec ($Re = 3 \times 10^4$ per ft) as it is the optimum speed for high quality dye flow visualization. The models were mounted in an inverted position on a forced roll oscillation rig (Figure 7). The drive mechanism used to oscillate the model is shown in Figure 8. The forced-oscillation rig had roll amplitude capabilities of ±50° and a frequency range of 0 to 0.22 Hz. This rig could also be held stationary for static condition tests. Both rigs were attached to an adjustable turntable which allowed up to 30° β_T in either direction. Angle of attack (or α_T) was adjustable up to 60°. The dye was pulsed manually by applying short pressure pulses to flexible dye lines. This simple technique was employed after a solenoid valve failed to accurately cut off the dye pulses.

Contrast levels were very important to the successful use of ExpertVision. Matte gray models with black "dots" for surface reference points and black dye packets seemed to be the best model/target combination. A black background was useful for easily isolating the model; however, if the dye travelled off of or past the model trailing edge, it was masked against the dark background. A photographically neutral (18% gray) background successfully provided a slight contrast between model and background while allowing a full view of the dye packets.

Lighting was highly configuration dependent. It was important to arrange the lighting so that few shadows or bright "hot spots," which would make accurate data reduction impossible, appeared in the video image. Arranging and rearranging light proved to be a very time-consuming task. Even with this extra care, there was

considerable data dropout during the forced oscillation tests because of lighting variations as the model rolled. Multiply-redundant cameras seem to offer a way to preclude this loss of data.

5.0 MODELS

Three models were constructed for the test, a NACA 2412 airfoil, a 70° delta wing, and an 80° delta wing. The airfoil had a 11.75 inch span and a 10 inch chord. Unfortunately, the resulting aspect ratio was too small to allow a sufficient length of two-dimensional flow. Transparent 1/8 inch plexiglass end plates were added to the model, but had little effect. The model itself was constructed of 1/16 inch sheet plastic ribs and skin, and had 16 dye ports.

The 70° sweep and 80° sweep delta wing models each were 10 inches in length and had a 25° single bevel cut from the lower leading edges (Figure 9). They were made from 1/8 inch aluminum and each had six dye ports, although only the forward two ports on each model were utilized. Originally, the models were painted glossy white; however, due to high contrast levels between the model and the background, the models were repainted to a flat medium gray. Flat gray and a photographically neutral (18% gray) background gave the optimum color contrast with black dye pulses.

6.0 INSTRUMENTATION

ExpertVision software owned by Texas A&M processes sequences of two-dimensional video images to acquire centroidal translations of objects to be tracked. The manufacturer claims that up to 200 discrete passive targets can be tracked simultaneously; experience has shown that at least 20 targets have been tracked simultaneously. Up to ten megabytes (about 20,000 frames of outline video data) can be stored in the Sun minicomputer memory. This digitized data can be interactively examined, analyzed, edited, and plotted from the computer console with customized commands internal to the ExpertVision. This tool is potentially very powerful and is particularly attractive for those applications where dynamic motions must be measured without intruding upon and altering test conditions, as in water tunnel and wind tunnel measurements. Eventually, the present two-dimensional capability must be expanded to provide three-dimensional motion descriptions. Motion Analysis Corporation is now marketing hardware and software to capture and process three-dimensional images. For this study, only the two-dimensional capability was used.

ExpertVision is a general purpose motion analysis tool which acquires, processes, and displays motion characteristics of a subject dynamic system. A schematic of ExpertVision components is shown in Figure 10. A photograph of some of the components installed at the tunnel test site is shown in Figure 11. The present VP110 video processor (a proprietary design of Motion Analysis Corporation) can acquire raw video data at frame rates of 60, 200, or 2000 Hz using one of three possible camera/VCR combinations. These data are treated by the video processor, which sends data to a host minicomputer with a printer/plotter and specialized software for tracking and analyzing the motions of multiple targets.

Such targets may be explicitly identified with active sources, such as light-emitting diodes (LED's); they may be cooperative but passive targets, such as retro-reflective tape; or they may be totally passive targets -- that is, parts of the image which are inherently bright or dark with respect to the background as were used in this study. The video-based images are collected in real-time, but tracking and subsequent analyses are performed later at an interactive graphics workstation. This post-test data analysis includes: (1) digitization of the frame-by-frame movement of the centroid of each target, (2) connecting these centroids to construct a path for each centroid, (3) numerical differentiation to obtain velocities and accelerations (either translational or rotational) of each target relative to a fixed point in the field of view or relative to another target, and (4) frequency domain analyses to identify dominant frequencies, power spectra, etc.

The Video Processor

The functions of the video processor are twofold:

1) To provide a first level of object recognition by identifying the "X" and "Y" coordinates of the outlines of the objects to be tracked; and
2) To reduce the size of the video data stream to the extent that it can be stored in real time on the hard disk of a microcomputer by eliminating those parts of the images of no use to the subsequent tracking algorithms.

These functions are accomplished, at high speeds, by a combination of analog and digital hardware. The analog data stream is first filtered by a user-controlled hybrid bank-pass filter which can be used to eliminate noise generated by the video taping process or uneven background illumination. This filtering is followed by one of two, hardware-based, edge detection procedures: "Absolute Thresholding" or "Dynamic Contrasting." Using either of these methods, the user can select any combination of horizontal or vertical edges to delimit the objects being tracked. In general, four-sided edge detection provides the highest precision when locating the centroids of objects. Digital pipelining, using high speed ROM's and RAM's, provides the system with an edge-detection capability for which a patent has been applied.

In order to obtain maximum temporal resolution from conventional (RS-170-type) video signals, a standard video camera is externally synchronized to provide a non-interlaced, 60-field per second image stream. This synchronization limits the vertical resolution of the raw video signal to 240 viewable lines, however, the overall vertical image resolution is improved significantly when statistical algorithms (described below) are used to locate target centroids.

The horizontal coordinates of target outlines are determined by a digital counter which measures the elapsed time between a horizontal "synch" pulse and a detected edge. It is the resolution (or frequency) of this counter which determines the horizontal resolution of the raw video signals. At this time, the inherent resolution of the video processor is 1 part in 1024, but only the most significant 8 bits (1:256) are used. Thus, the perimeters of targets are established with a raw video resolution of 256 horizontal pixels by 240 vertical pixels.

The Computation and Properties of Centroids

Digitized video data are stored in a disk file as a series of frames (fields) ordered in time. The data for a single frame consist of a list of pixels which identify edges detected by the video processor. With the video processor properly adjusted for a given application, the list of pixels delimits the targets to be tracked.

A basic analysis of movement requires that targets (which are represented as sets of mutually "connected" pixels) be tracked through space and time. The first stage in this process is performed by a program (CENTROID) which, within each frame, segments the collections of pixels into distinct objects and calculates the geometric center (or centroid) of each target. The second stage entails tracking these targets through time. A second program (PATH) gathers the instantaneous centroid positions together to produce coherent trajectories for the individual objects. PATH is primarily a sorting procedure in which various centroids are assigned to specific trajectories. Consequently, spatial resolution, precision, and accuracy of the motion parameters are largely dependent upon the computation of centroids, and the statistical properties of these centroids.

Within each frame of digitized video data, the CENTROID program begins by centering a user-defined rectangular "neighborhood" over an arbitrary pixel and identifying all pixels within that neighborhood. All such pixels are then assigned to the image of a single target. Similarly, identical neighborhoods are established for each of these pixels, and the process is continued to exhaustion. At this point, no further pixels are within the associated "neighborhoods" of the connected pixels.

The "neighborhood" concept provides a "connectivity" criterion based upon a height and width specified (in pixels) by the user, however, each group of pixels identified in this manner must consist of a (user-specified) minimum number of pixels before it represents a target to be tracked. If the number of pixels accumulated is greater than or equal to the minimum, then a centroid location is determined by averaging the "X" and "Y" coordinates of the individual pixels forming the group. Clearly, a single centroid can be localized with greater than one-pixel precision because the average of a set of integers is generally a rational number.

In any video system, relatively low levels of noise produce minor fluctuations in the intensities of edges, and it is inevitable that occasionally such fluctuations will cross the threshold for edge detection. Consequently, digitized boundaries of stationary objects may vary from one frame to the next. Such "pixel twinkle" may be reduced, but not totally eliminated.

In addition to the ExpertVision hardware, two high speed VHS format video cameras, for planform and side views (Figure 7), were used to record the taped data. Two quartz and two photo studio flood lamps were used to light the model and background.

7.0 DATA ACQUISITION AND ANALYSIS PROCEDURES

All video data for these experiments were collected on standard 0.5 inch VHS video cassettes. Data were reduced only from cassettes recorded in monochrome (black and white) mode, though some flow visualization tapes were made with a separate color camera owned by Eidetics for comparison purposes. None of these color tapes were processed at Texas A&M with ExpertVision.

Each test was photographed from both the side and the bottom (top or planview of the model) of the water tunnel with video cameras arranged orthogonally. Since each view of the model represents a plane, three-dimensional movement of a vortex can be obtained by correlating the two data planes together with the X water tunnel axis as the common dimension. To make this correlation, the user must use considerable judgement to guarantee that the two views are time-correlated. Despite the lack of a synchronization unit for the two cameras, a fairly good time-correlation was achieved by manually editing the data to insure that the same individual dye pulse was tracked in each view when digitizing the data. Since the dye pulse appears simultaneously in both camera fields of view, it serves as the initial frame for each of the two video files. After the first point has been time-matched manually, the remaining frames are automatically synchronized since the frame rates of the two cameras are identical (60 Hz for the August 1987 tests and 200 Hz for the October 1987 tests). While this procedure was successful, the use of an automated software program that automatically marks and correlates three-dimensional coordinates would greatly improve the efficiency of this time-consuming and tedious process. Moreover, redundant cameras recording the same scene could provide a statistical basis for improved accuracy for the centroiding process.

Once a desired segment of video tape is identified, recorded images are played back using a standard Panasonic 60 Hz video recorder to input the video imagery to the Motion Analysis VP-110 Video Processor for filtering, masking, edge detection, and analog-to-digital (A/D) conversion processes. The VP-110 allows the user to establish a gray scale threshold so that the edges of the target of interest are determined. To facilitate identification of the targets, the model and the background were a light gray while the dye injected into the vortex core was black. It is these edges created due to the contrast of the target and background which are A/D converted for further digital processing on the Sun 2/130 computer. The VP-110 allows the field of view in a video frame to be selected for digitization by adjustable masking functions as well as the elimination of unwanted information through filtering and thresholding to improve upon the signal-to-noise ratio.

ExpertVision software on the Sun 2/130 is used to interface with the VP-110 and the video recorders to create the digitized video file on the Sun computer. Camera frame rates, length of video tape to be digitized and selection of frame increments are interactive user inputs to the software package used in creating the raw video file. After digitization of the raw video file, several other software modules are available in ExpertVision for editing raw data, centroiding targets, generating target paths, extracting path velocities and accelerations, and determining X and Y or X and Z path and velocity components. The user can also enter scaling dimensions

directly into the data reduction packages, using a mouse and reference points placed in the field of view. For these tests, black circular dots were painted on the gray model at known distances apart for reference points.

Despite careful filtering, masking and thresholding, each raw video file still requires moderate to extensive user intervention to edit unwanted information from the field of view. Frame by frame editing, a very tedious process, was required to insure accurate tracking of only the desired targets. It was this phase of the data reduction which was extremely time-consuming, but absolutely crucial to the quality of the results obtained. Once a clean video file was obtained with this detailed editing process, the centroid module was used to accurately determine the centroids of the targets from the edges displayed in the video file. Next, the PATH module created the trajectories by connecting target centroids in adjacent time frames. In the oscillation tests, both the paths of the wing as well as movement of the vortices and movement of the vortex burst points were simultaneously tracked to accurately correlate vortex movements and wing motion. For example, in this case, the output of the PATH function is a planar trajectory of the target(s). The speed function was then used to determine the path velocity as a function of time for each target. The path file could also be split (with the SPLIT module) into X and Y velocities or into X and Z velocities. Of course, this same function could also be used to resolve positions along any of the coordinate directions.

The vortex flows were visualized in these water tunnel tests by injecting both continuous dye streams and pulsed dye elements. Continuous dye filaments were very useful in quickly determining vortex trajectories and burst points. This process required that only a few frames of data be digitized, edited, and analyzed for those test segments with a stationary mode. Continuous dye streams were also needed to accurately track vortex burst point movement in conjunction with wing motion; however, the editing required for this facet of the data reduction was extensive. Pulsed dye packets were essential to determining the velocity and acceleration associated with these vortical flows. Individual elements of fluid had to be tracked from frame to frame, and frame-by-frame editing made this part of the data reduction very demanding. These tests also provided burst point information but at a much higher cost in time than did the continuous dye streams. These files also required extensive editing to eliminate extraneous or unwanted information from the field of view.

8.0 DISCUSSION OF RESULTS

Table 1 shows the test matrix for both the 70° and 80° wing models for stationary and forced oscillation experiments. The following discussion will first address results for the stationary models and then for the forced oscillation models.

Stationary Model

Each model tested was first mounted in the test section without motion and aligned as described in the section on Test Techniques. Dye was injected into one or both dye ports near the apex of the delta planform so that when the dye entered the

water stream it was immediately captured in the leading edge vortex for the appropriate side. The initial portions of any specific run (at a given flow condition and model orientation) were devoted to simply observing the location and stability of the pair of vortices and the burst points. Video tape was then taken of this steady flow field. The steady, continuous dye stream from this first part of the taping sequence was particularly helpful in ascertaining burst point locations. The vortices themselves were quite stable in location, varying no more than a few pixels. However, it was obviously easier to define the angular displacement of the vortex core from surface of the model ($\alpha_T - \alpha_c$ in Figure 12a) from the side view camera and the displacement of the vortex cores from the leading edge of the model ($\theta - \theta_c$ in Figure 12b) from the video camera positioned on the floor looking up through the bottom of the test section. This manual process of correlating information from the two cameras is highly approximate and does not utilize statistical redundancy to refine measurement accuracy within the system.

Vortex Location. The vortex locations defined in the manner described above with the data processed by ExpertVision were repeatable and showed little variation from run to run at the same conditions. Figures 13a and 13b summarize the two location parameters for all α_T tested for the 70° wing. The data show vortex core locations above the wing in fairly good agreement with both theory[1,2] and with previous experimental measurements [3,4]. The largest discrepancies are at low α_T.

Vortex core sweep angle data are show in Figure 13b. These data generally show lower sweep angles than reported by Erickson[3] or Lambourne and Bryer[4] in other water tunnels. These new data seem to come closer to theoretical predictions, particularly those of Brown and Michael[1].

Vortex Burst Points. The average burst point locations for the runs described in the previous section are shown in Figure 14. They are presented for the 70° and 80° delta wings as a function of α_T. The model root chord (c) is used as a reference length to nondimensionalize burst point locations. For the 70° delta wing, vortex burst points occur behind the trailing edge at α_T below 25°. They are outside the video field of view and therefore cannot be digitized. For identical reasons, no burst point locations are available below α_T of 35° for the 80° delta wing. As expected, the burst point moves toward the leading edge as α_T is increased. However, the vortex breakdown positions from these tests are considerably further forward than have been measured previously[5,6]. A small, but representative sample of these other measurements are shown in Figure 14. Once again, it appears that a bias has been introduced into the data, perhaps because of uncertainty in setting α_T. In any event, additional study is needed to determine the reasons for these differences.

Figure 14 actually summarizes a number of runs. It presents the average locations for left and right vortices; Table 2 shows how asymmetries in model mounting, i.e. a slight roll (Φ) or yaw angle (β_T), result in asymmetries in the vortex measurements. These anomalies are seen by examining both the vortex burst points and the vortex core angles, measured from the mean flow direction in the X-direction. If the model

were symmetrically mounted with a true $\beta_T = 0°$ and $\Phi = 0°$, the vortex burst points and θ_c should be the same for both left and right vortices. (This property appears at $\alpha_T = 30°$ or less for the 70° delta wing model fixed in the tunnel.) Runs 14 and 62 with $\alpha_T = 30°$ for this wing, clearly show the alignment difficulties. Run 14 has a left vortex burst point of 4.63 inches compared to 5.21 inches for the right vortex. The likely cause was a slight β_T (or perhaps a small Φ). Here, the left vortex is the windward vortex. The azimuth angles (θ_c) are very close between the two sides. Run 62 shows a much more asymmetric flow where the left vortex bursts farther back than the right vortex. Also, θ_c for the right vortex is about 2.4° greater than for the left one. These angular positions correspond to a β_T (or a Φ) in the opposite direction, where the right vortex is the windward vortex. Also, note that the average vortex burst point is 4.92 inches for run 14, compared to 4.65 inches for run 62, a difference of 5.6%. The average θ_c of runs 14 and 62 are 11.94° and 12.08°, respectively, a difference of only 1.2%. Despite asymmetries in the burst points and azimuth angles between individual runs, the average values are fairly repeatable from run to run. Differences in these values could also be explained by slight differences in the α_T due to uncertainty in that alignment. This uncertainty and/or lack of repeatability in vortex burst point location was noted visually during the tests also. The video data simply corroborate this observation. At least part of this uncertainty can be attributed to asymmetry in the model mounting arrangement, in the model itself, in the test section flow field and/or in the data reduction procedures. This difficulty in obtaining repeatable vortex burst points for nominally identical test conditions needs to be analyzed in future development of the measurement scheme. However, there is no indication that the video data collection equipment played a significant role in the alignment uncertainty. In fact, the digitized data support visual observations made during the test and provide a basis for reducing alignment errors in future tests.

The effect of flow asymmetry on vortex burst point locations is readily observed and quantified using ExpertVision. Average values of the burst point locations for a representative set of asymmetric flow conditions is plotted in Figures 15 and 16.

Figure 15 shows more directly how both leeward and windward vortices are affected by increasing crossflow. These data are all for the 70° delta wing. Two different model angles of attack are presented and the burst point locations are plotted against β_T. The windward burst point varies almost linearly with β_T, moving very near the leading edge. Again, the vortex that is generate at $\alpha_T = 25°$ moves the burst point well aft. The leeward vortex does, however, apparently gain considerable burst point stability from being more nearly aligned with the flow, since it bursts further downstream. No bursting occurred over the video field of view for the leeward vortex at $\alpha_T = 25°$ and $\beta_T = 10°$; the burst point is downstream of the trailing edge of the model on that side.

Figure 16 compares the burst point behavior for both wings at $\alpha_T = 35°$ for the same range of β_T as considered above. The leeward vortex burst point is not

shown for the 80° wing because, again, it bursts behind the trailing edge of the wing outside the field of view. Once again, the vortex burst point is moved aft, apparently affected more by the leading edge sweep angle than α_T.

Vortex Core Velocities. The velocity of fluid element trapped in the core of the vortex was one of the primary measurement goals for this feasibility phase. The video tracking of dye pulses, the algorithms used in ExpertVision, and the editing processes evidently provide reasonable estimates of the velocity in the core of the vortex. Figure 17 summarizes typical data collected for the 70° sweep model at four different α_T's. Measured velocities are nondimensionalized by the freestream velocity of the tunnel, 4 inches per second. (The video system was used to check tunnel speed at several different speeds and in every case, the measurements were very close to the speeds set by Eidetics personnel and measured in the test section.) Time is also nondimensionalized in this chart with the nondimensionalizing denominator based on the length of time it would take for a fluid element having freestream velocity to travel the reference length (c). As expected, the maximum velocity increases with increasing α_T, reaching a peak value of approximately 3 times that of freestream at $\alpha_T = 35°$. Erickson[3] reported core velocity ratios ranging from 2 to 3 at angles of attack of 30° to 40°. These velocities were also dependent to some extent on Reynolds number of the tests. The data collected and reduced with this method certainly fall within this range, though more detailed comparisons need to be made. Moreover, the measurement scheme suggests that the fluid does not attain this speed until some time elapses. At least an approximate acceleration can be inferred from the velocity data in Figure 17. The data, especially for $\alpha_T = 25°$, show that core velocity is not uniform. The oscillatory character may be due to the dye path being slightly outside the center of the vortex core. The oscillations would then reflect the helical motion when recorded on the two-dimensional video image. This particular point illustrates one of the reasons a third dimension with four cameras is essential to make ExpertVision more useful as a tool to study such motions.

Vortex Core Accelerations. ExpertVision also allows accelerations to be derived directly by numerical differentiation of the velocity profiles illustrated above. The results are depicted in Figure 18. These data reflect the oscillations in the velocity but still offer useful insight about the acceleration of the fluid in the vortex core. At least the major features stand out. The initial acceleration of the dye element, as it comes out of the dye port, is shown in the first 0.04-0.05 nondimensional time units. Moreover, the deceleration of the fluid element at about 0.34 $\dagger/\tau$ pinpoints the vortex breakdown. Finally, an average deceleration of the fluid in the vortex core throughout its passage down the tunnel is apparently shown from about $0.15 < \dagger/\tau < 0.63$. This average deceleration, ignoring the spike at $\dagger/\tau = 0.34$ that is associated with vortex breakdown, is about 5 ips^2. Perhaps this deceleration represents dissipative forces in the fluid flow field. Recognizing that numerical differentiation is a process that loses information, the acceleration algorithms in ExpertVision still provide useful information about acceleration trends. Considerable further development effort is needed to improve and automate the data reduction process for extracting accelerations.

Forced Roll Oscillations

All of the measurements discussed in the preceding paragraphs were made with the model fixed in the water tunnel. However, the video camera gives a water tunnel experimentalist more capability to make dynamic measurement. Delta wings provide classic examples of the nonlinear aerodynamics associated with vortical flow structures. This measurement tool allows the researcher to quantify and catalog the relationship between the motion of the lifting surface and its associated vortices. Both amplitude and phasing relationships can be studied in detail. To demonstrate this capability, the forced oscillation rig described previously was set to produce $\Phi_T = \pm 30°$ at three different oscillation frequencies. Again, both steady dye streams and pulsed dye streams were used to locate burst points and to calculate velocities of fluid elements trapped in the vortex core. These measurements provide a good indication of the capability of this video-based measurement scheme to capture and quantify the fluid motion in this crucial part of the flow.

Movement of the Vortex Core. Visual observation of the movement of the vortex cores during a forced roll oscillation reveals that the fluid in the core tends to remain fixed in space initially. After some time lag, the core is apparently influenced by the pressure field around the moving wing and begins to follow the rolling motion. However, there is a noticeable lag in the movement of the vortex. On the upward-moving side of the model, the vortex is typically further from the model than it is for the fixed model at the same α_T. Conversely, once that side of the wing starts the downstroke, the vortex does not immediately reverse direction. Consequently, for most of this part of the cycle the vortex lies closer to the lifting surface than when the wing is not moving. No attempt was made to quantify these displacements, though it appears to be possible. Instead, the relationship between burst point location and roll angle and the relationship between core velocity and roll angle were the focus of the data reduction. Figure 19 shows a sketch illustrating the definition of terms used in the next two sections.

Movement of the Vortex Burst Point. One of the most interesting features of the vortex-model interactions noted during these forced roll oscillations was the relationship of the vortex burst points to Φ. For the lowest frequency (Figure 20), as the model rolled toward a vortex, the burst point moves toward the leading edge after a short time delay. When the roll direction reverses, again after a time delay of approximately 0.1T, the burst point moves aft. For higher frequencies (Figures 21 and 22), however, the time delay grows and completely alters the picture. In the two higher frequency forced oscillations the burst point is still moving forward as the wing rolls away from the vortex. It appears that the time delay between movement of the lifting surface and movement of the vortex core is a very important factor in this relationship and therefore may be the key to predicting this motion. The important point, for the purposes of this feasibility study, is that with ExpertVision this behavior can be readily quantified. Both the time delay and the amplitudes of the burst movement for a given forced roll oscillation frequency are part of the information collected. Figures 20 - 22 show such data for the 70° wing operating at $\alpha_T = 25°$ for three different frequencies. The vertical axis in these

plots is the burst location minus the mean burst point location at $\Phi = 0°$ (which was 4.66 inches from the model apex for these test conditions). The period of the burst point oscillation is very nearly the same as that of the roll oscillation.

The amplitude of burst point movement was observed visually to diminish as the frequency of the forcing function increased. The video data quantify and confirm that qualitative observation, with the peak amplitudes decreasing as shown in Figure 23. The trends in this plot certainly follow the qualitative observations and suggest that at an infinite frequency of oscillation, the vortex burst points would remain fixed. The data raise questions about where the vortex system would be located (relative to its static position) and whether or not the strength of the vortices are affected by rapid rolling oscillations. Of course, the purpose of these tests was to show the potential for the measurement scheme, not to make such detailed measurements. The ability to obtain such numerical measurements with an automated system, though, makes it easier to ask such questions with a reasonable hope of being able to answer them without complex and/or intrusive measurement tools.

Phasing Between Roll Angle and Vortex Burst Point Location. The phasing between movement of the model and movement of the burst point can also be extracted from Figures 20 - 22. This phase difference is shown in Figure 24. If this phase increment is taken as the fraction of the roll oscillation period between the axis crossings shown in each of these plots, the resulting data also show trends that corroborate qualitative observations. At low frequencies the burst points take on the values associated with the mean position. In Figure 24 this behavior is indicated by the phase differences tending to either 0 or 1 (that is, with the wing fixed, there is no phase difference or 360° phase difference). However, the phase shift quickly becomes about 20% of the oscillation period as the nondimensional oscillation frequency is increased. If the oscillation frequency increases, the phase shift increases. However, the rate of increase drops off drastically. Obviously, to completely define these curves, forced oscillations at several more frequencies must be done. Nonetheless, the capability of this video-based motion analysis tool to produce useful and thought-provoking quantified data is apparent.

Vortex Core Velocities in a Forced Roll Oscillation. The capability of the system to measure fluid velocities at given streamwise locations during a forced roll oscillation is illustrated in Figure 25. Obtaining these velocities was tedious and required video taping the test section at a higher camera sample rate (200 Hz rather than 60 Hz). This higher sample rate and the resulting large data files significantly multiplied the data reduction effort required. Furthermore, since the vortex core was itself oscillating and since it was more diffused, tracking of individual fluid dye packets was not always possible. To date, a complete oscillation cycle could not be digitized reliably because the vortex away from the side camera was not visible and could not be used for data. So far, no planview video has been found that continuously allows tracking of the vortex. The vortex nearest the side camera, the left vortex, essentially dissipated when the model reversed direction and the left wing started moving upward. Attempts are still being made to extract these data from the planform view, but so far to no avail. For this reason Figure 25 includes only data for the left vortex during the part of the roll

oscillation when the left wing was moving down. These difficulties lend further support to having redundant cameras, not just two orthogonally mounted ones, to collect the video images.

A statistical ensemble of measurements is needed to obtain these velocities. This statistical ensembling is very tedious and is not automated at all in the current two-dimensional version of the software. These data required 20 to 30 times the computer time and manpower to produce than had been originally estimated. This type of statistical process needs to be programmed into the data reduction system with specifically tailored ExpertVision subroutines. Since the software is UNIX-based, it lends itself to such modifications and, indeed, they will be necessary if such data acquisition is to be a routine part of water tunnel testing. Nevertheless, when these difficulties were overcome (with considerable manual editing of the files and generous application of engineering judgement in interpreting the data), the results appear to be quite consistent.

The measured core velocities decrease at any given location during the downstroke. In fact the change in velocity at any of the three streamwise locations is very nearly linear during this part of the oscillation. At all three locations the velocity decreased approximately 1.5 ips during the 30° downstroke of the model. It is also interesting to note that the velocities at 0.25c and 0.4c are virtually identical. The curves are remarkably regular and smooth, lending some credibility. However, the authors are still searching for both theoretical calculations and/or other experimental results with which to compare these measurements. So far none has been found.

Even though these data look rather promising, core dynamics make these velocity measurements somewhat questionable. The core velocities should be measured in three dimensions since the vortices were observed visually to be moving in all three directions as the forcing motion of the wing model was imposed on the vortex system. These data are another example of the need for three-dimensional measurements if the video data are to provide more detailed data for analysis of vortical flow structures.

9.0 CONCLUSIONS AND RECOMMENDATIONS

In this section, the major conclusions derived from this short conceptual study are stated and tied to specific recommendations wherever appropriate. The authors have attempted to order these conclusions and recommendations in order of importance with the most important ones first.

Conclusions

A surprising amount of data quantifying the fluid dynamics of a much-studied generic and three-dimensional vortical flow problem in wind tunnels and water tunnels were produced from two short tunnel entries. Some of the results give numbers to properties not heretofore published to the knowledge of the authors. However, it was not the purpose of this short study to exploit the use of ExpertVision or a similar video-based system for use with water tunnels. The only

purpose was to demonstrate the potential of the system for further development as a nonintrusive means of obtaining data in a water tunnel. Thus, the overriding question to be answered was:

> Does the system show sufficient promise to warrant further development? To this question, all the data show the answer to be: yes!

The mere fact that so much information was collected even as the experimenters were learning how to use the system is a clear indication of how much potential the system has for studying fluid dynamics. It would be a serious mistake not to expand this potential and improve upon the techniques used in this initial work. (R1)

One of the most serious deficiencies in the video tracking scheme is that in its present form it collects data in only two dimensions. This shortcoming means that asymmetric motions, like the forced roll oscillations, cannot be fully represented in the data output. Moreover, the full power of statistical techniques with redundant measurements from multiple cameras cannot be fully utilized to improve the accuracy of the measurements. This shortcoming was highlighted in the discussion of several of the data plots where there was distortion due to the planar nature of the basic data collection schemes. No automated ties between the motion of the same fluid element as seen by each of the two cameras could be developed with this software. Three-dimensional measurements must be added as one of the first priorities in further development of the scheme. (R2)

The data reduction software, especially the editing processes, are much more time-consuming than was originally thought. Special purpose macros, especially those which will better automate the editing process and carry out statistical correlations without user-intervention, must be coded and verified. (R3)

Repeatability of static tests was imperfect, probably because of small flow asymmetries introduced either by the size of the tunnel test section, slightly asymmetric flow, or most likely, uncertainty in the model alignment procedures. The limited comparisons completed to date suggest that either the alignment procedures and tunnel flow characteristics are contributing to static measurement errors or else the data reduction procedures need to be altered. It appears that ExpertVision can be used to help in this alignment calibration, but the software tools for doing so need to be developed. Further integration of the software, hardware, and the procedures for setting model angle of attack, yaw angle, and roll angle are clear needs. (R4)

The data obtained from these tests could not be fully verified and confirmed with other available experiments or with computational results. The general trends, though, are quite consistent. (R5)

Recommendations

Based on the conclusions listed above, the following recommendations are offered. Again, these recommendations are listed in rough order of priority and numbered

to correspond with the numbers indicated in parentheses (R1, R2, etc.) in each paragraph of the conclusion section.

(1) It is strongly recommended that Phase II effort jointly proposed by Eidetics International and Texas A&M University be funded to develop this scheme for nonintrusive dynamic measurements in the water tunnel.

(2) The top priority in this continued development ought to be expanding the system to three-dimensional capability by purchasing the upgraded software now offered by Motion Analysis Corporation and additional hardware that has at least some of the improvements needed.

(3) Improvements to the data reduction software must be sought that will (a) allow cross-correlation between multiple cameras so that redundant measurements of the same motion can be used, (b) streamline the editing process so less frame-by-frame editing is necessary, and (c) automate more of the specific processes unique to data collection in the water tunnel.

(4) The water tunnel support equipment should be further improved with emphasis placed on those items that have the best chance of reducing flow alignment uncertainties.

(5) A comprehensive search of the literature to locate a more complete set of comparison data is recommended for the second phase of the development. Other type of measurements, like those made with a laser doppler velocimeter in similar experimental conditions would be the most desirable form of verification for the process. Data must be reduced further and put into forms where it can be compared directly to both other experiments and to theory.

Summing up, the ExpertVision video-based approach to motion measurement has demonstrated a unique potential for making nonintrusive measurements in the water tunnel. It is relatively low-cost, easy to learn, and even in its two-dimensional form, yielded a considerable amount of useful quantitative data for a moderate investment of time in data reduction and required attention to detail (lighting, camera placement, camera settings, and the like) during testing. It is strongly recommended that this system be developed further as a tool for collecting and reducing water tunnel data.

10.0 REFERENCES

1. Brown, C.E. and Michael, W.H. Jr., "On Slender Delta Wings With Leading-Edge Separation," NACA TN 3430, 1955.

2. Smith, J.H.B., "Improved Calculations of Leading-Edge Separation From Slender, Thin Delta Wings," Proceedings of the Royal Aeronautical Society A. 306, 1968, pp. 67-90.

3. Erickson, G.E., "Vortex Flow Correlation," AFWAL-TR-80-3143, January 1981.

4. Lambourne, N.C. and Bryer, D.W., "The Bursting of Leading-Edge Vortices -- Some Observations and Discussion of the Phenomenon," Aeronautical Research Council TR-RM-3282, London, 1961.

5. Moore, W.A., Erickson, G.E., Lorincz, D.J., and Skow, A.M., "Effects of Forebody, Wing and Wing-Body-LEX Flowfields on High Angle of Attack Aerodynamics," SAE Paper 791082, December 1979.

6. Nelson, R.C., "Flow Visualization of High Angle of Attack Vortex Wake Structures," AIAA Paper 85-0102, January 1985.

11.0 TABLES

TABLE 1
Non-Intrusive Flow Measurement
Test Matrix

Model: 70° Delta Wing

α_T	β_T	f	ø	Run Type
10	0,±5,±10	----	----	Stationary
15	|			|
20				
25				
30				
35				
40				
15	0	0.0440	±30	Forced Oscillation
25	|	0.0179		|
		0.0440		
		0.1760		
35		0.0440		

Model: 80° Delta Wing

α_T	β_T	f	ø	Run Type
15	0,±5,±10	----	----	Stationary
20	0,±5			|
25	0,±5,±10			
30	0,±5,-10			
35	|			
40				
25	0	0.018	±30	Forced Oscillation
	|	0.044		|
		0.174		
35		0.044		

Table 2. Uncertainty in Burst Point Locations
(70° delta wing Yaw Angle: 0° Roll Angle: 0°)

Run No.	Angle of Attack	Left Vortex Burst Point	Right Vortex Burst Point	Average Burst Point	Left θc	Right θc	Average θc
40	10	Behind Wing	Behind Wing	Behind Wing	10.0	12.5	11.25
35	10	Behind Wing	Behind Wing	Behind Wing	13.14	9.6	11.34
45	15	Behind Wing	Behind Wing	Behind Wing	10.76	12.25	11.5
36	15	Behind Wing	Behind Wing	Behind Wing	13.9	10.3	12.1
81	20	8.4	Behind Wing		10.4	12.99	11.7
02	20	Behind Wing	Behind Wing	Behind Wing	10.66	12.72	11.69
56	25	5.924	7.232	6.578	10.99	12.51	11.75
09	25	6.329	7.074	6.702	12.71	11.24	11.98
62	30	5.715	3.585	4.65	10.9	13.26	12.08
14	30	4.63	5.21	4.92	11.93	11.95	11.94
67	35	2.341	2.719	2.53	10.76	13.86	12.31
19	35	3.153	2.452	2.803	10.86	13.20	12.03
72	40	1.219	1.215	1.217	13.16	10.45	11.8
77	40	1.204	1.20	1.202	12.14	10.11	11.57

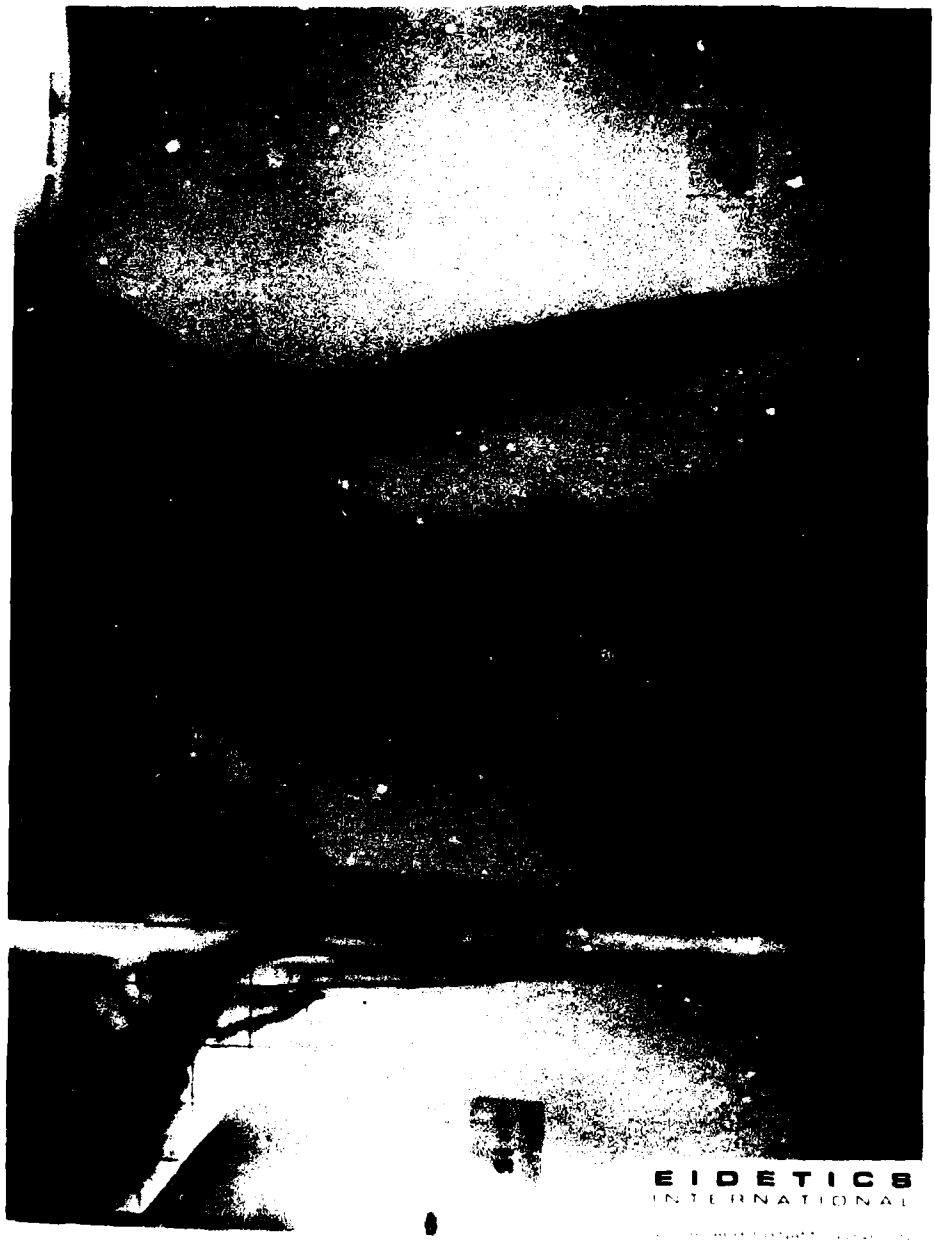

Fig. 1 - Water tunnel fow visualization of a generic fighter model.

EIDETICS INTERNATIONAL
AEROEIDETIC RESEARCH LABORATORY

FLOW VISUALIZATION WATER TUNNELS

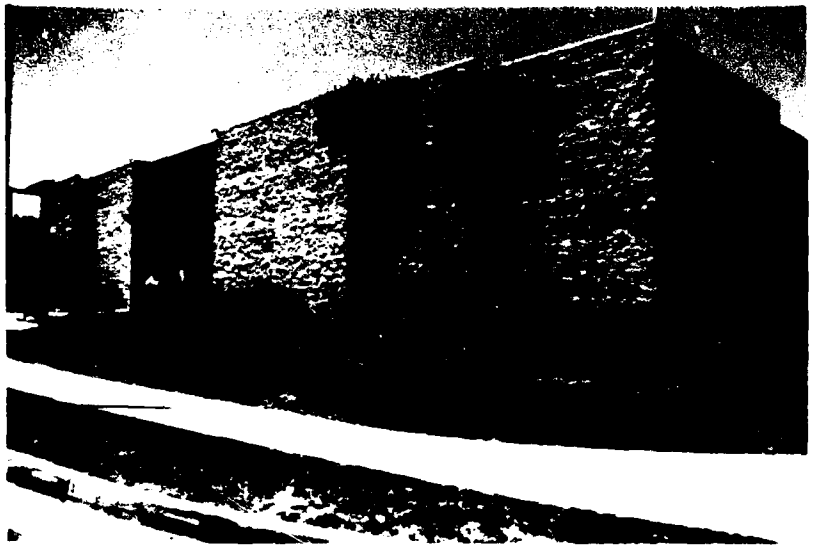

EIDETICS FACILITY

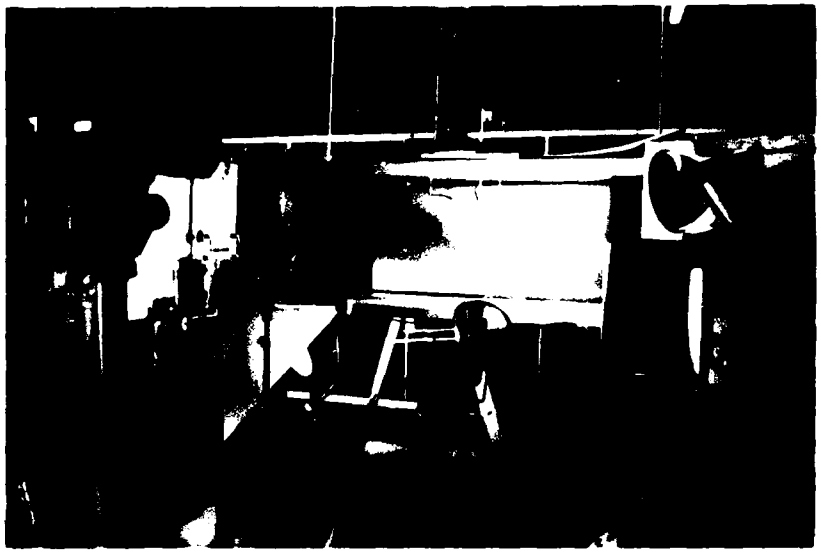

MODEL 1520 TEST SECTION

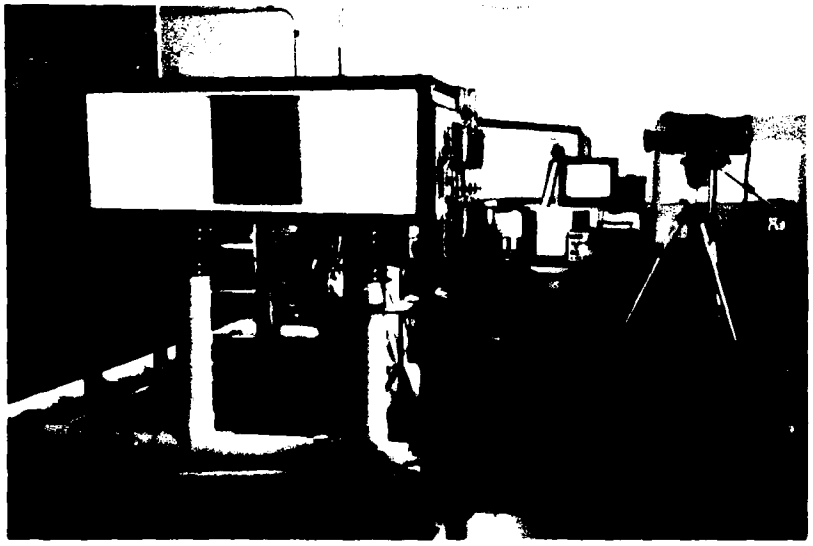

DOWNSTREAM VIEWING WINDOW

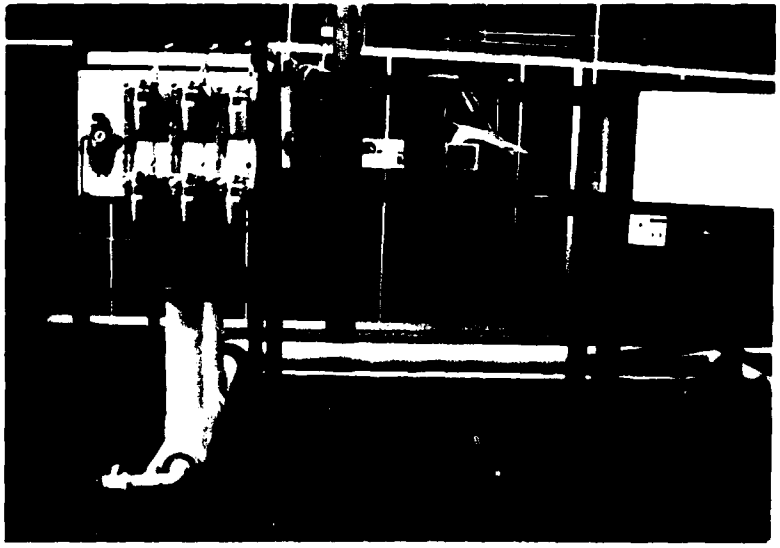

TEST SECTION/DYE SYSTEM

Fig. 2 - Eidetics Flow Visualization Water Tunnel

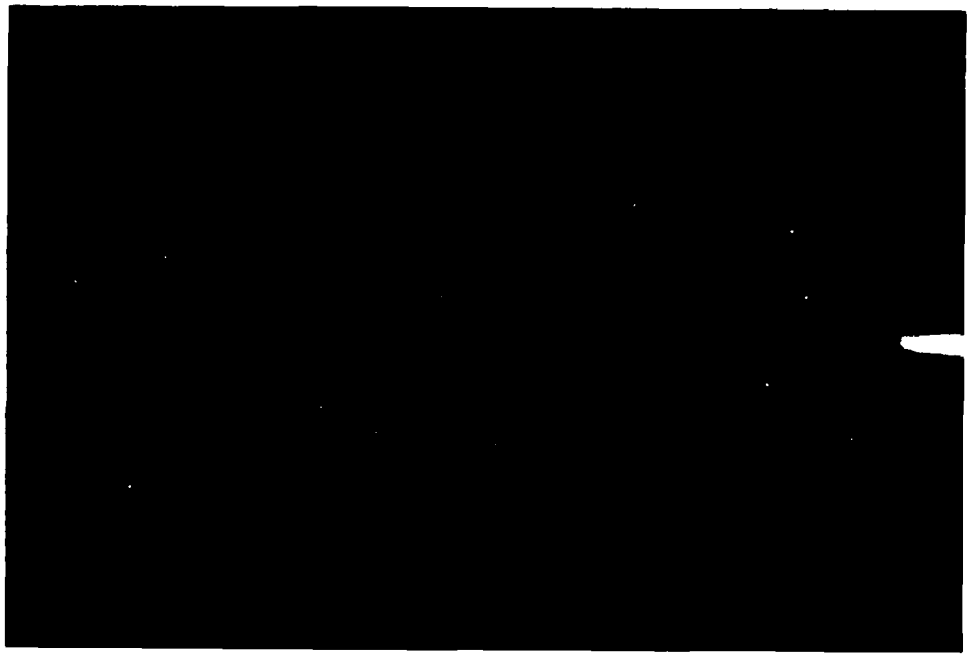

(a) Planform view

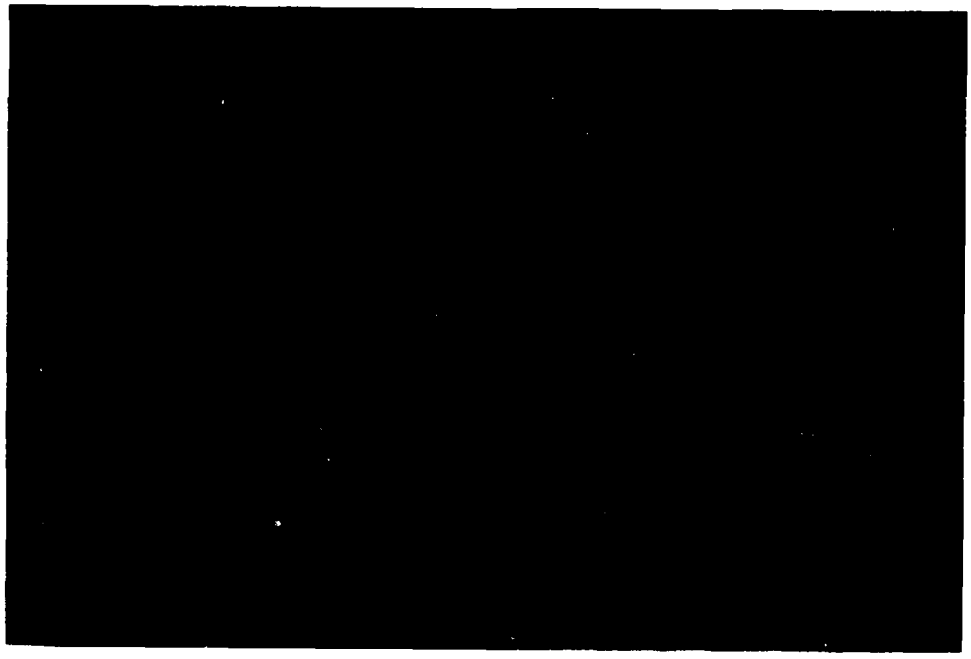

(b) Side view

Fig. 3 - Water tunnel flow visualization of a delta wing with continuous dye flow.

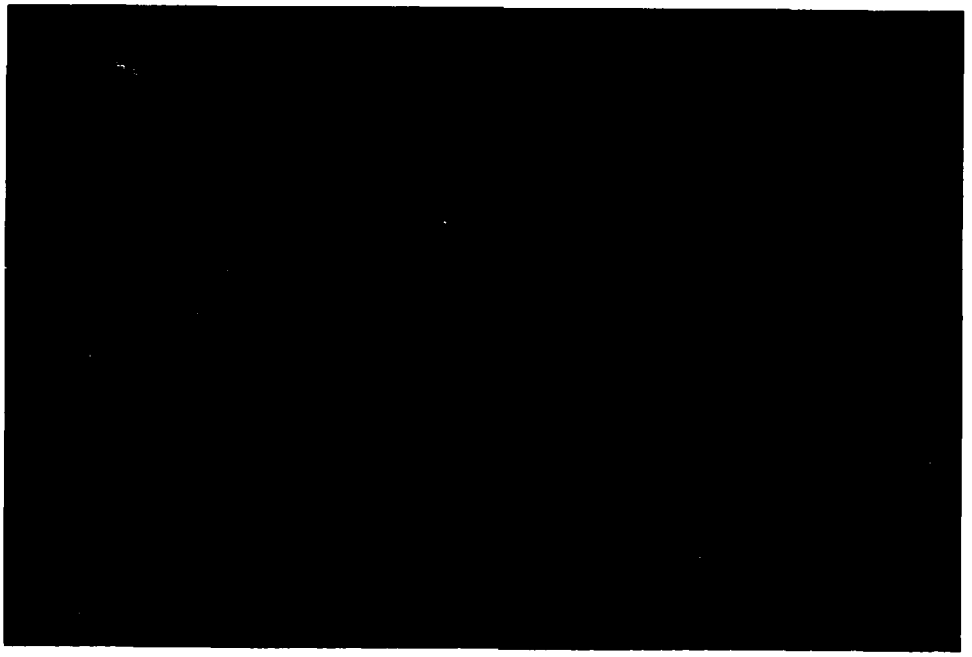

Fig. 4 - Water tunnel flow visualization of delta wing with pulsed dye flow.

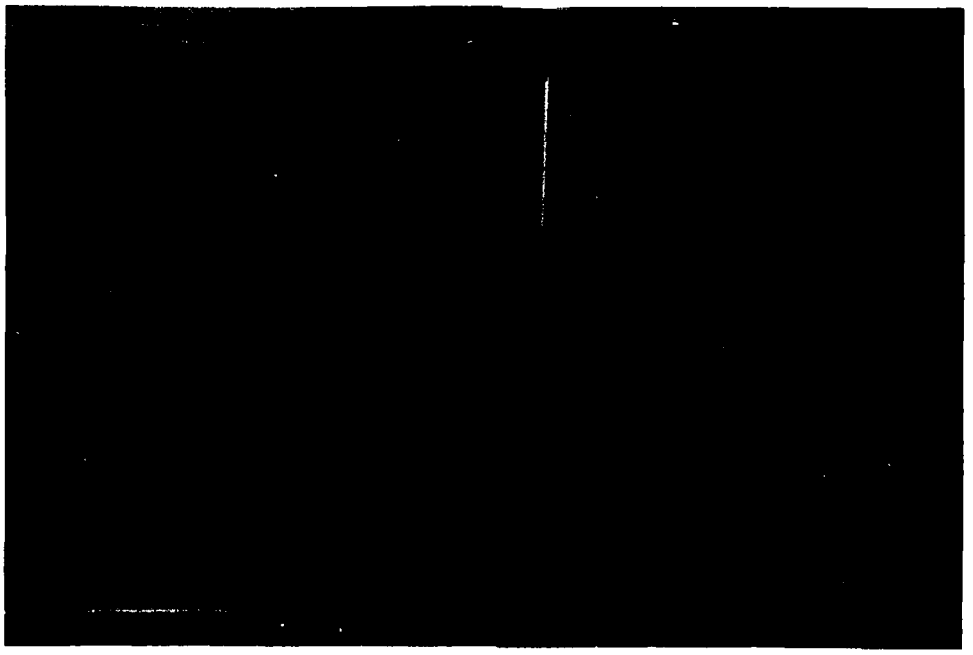

Fig. 5 - Delta wing model mounted on forced-roll apparatus in water tunnel test section.

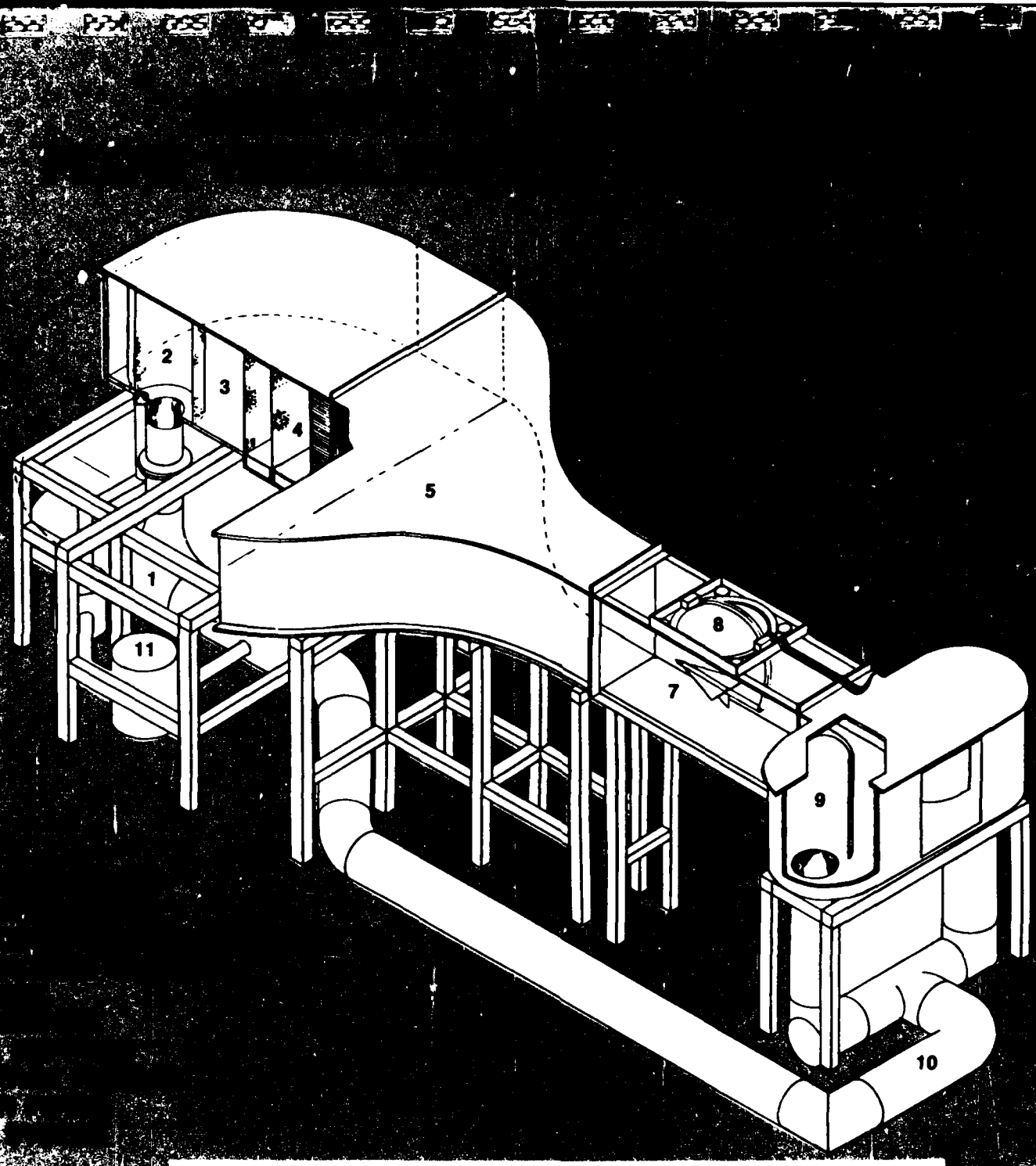

Fig. 6 - Schematic of Eidetics Model 1520 Water Tunnel

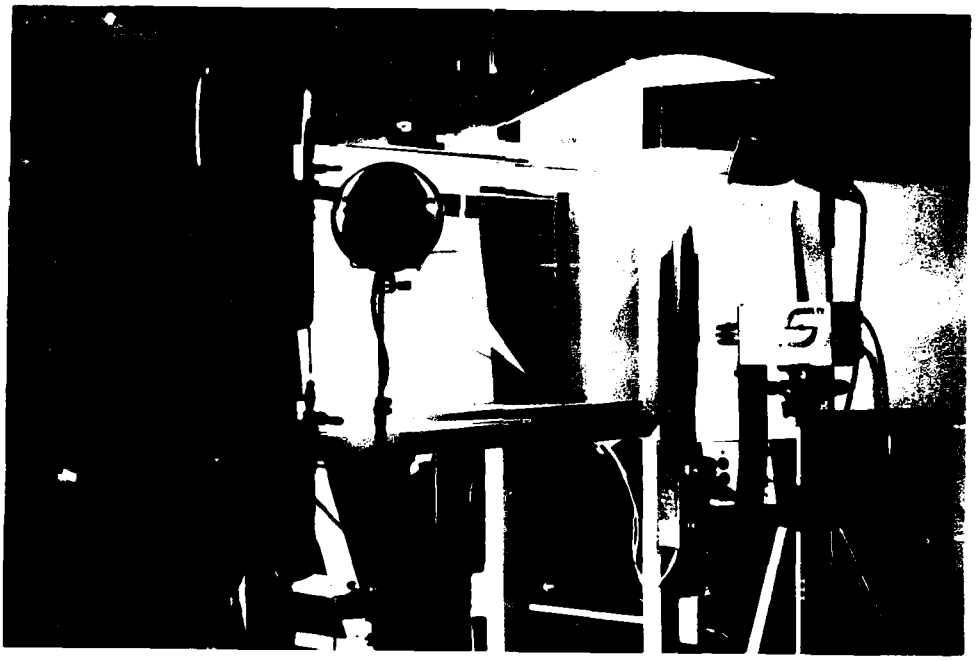

Fig. 7 - Water tunnel and ExpertVision instrumentation.

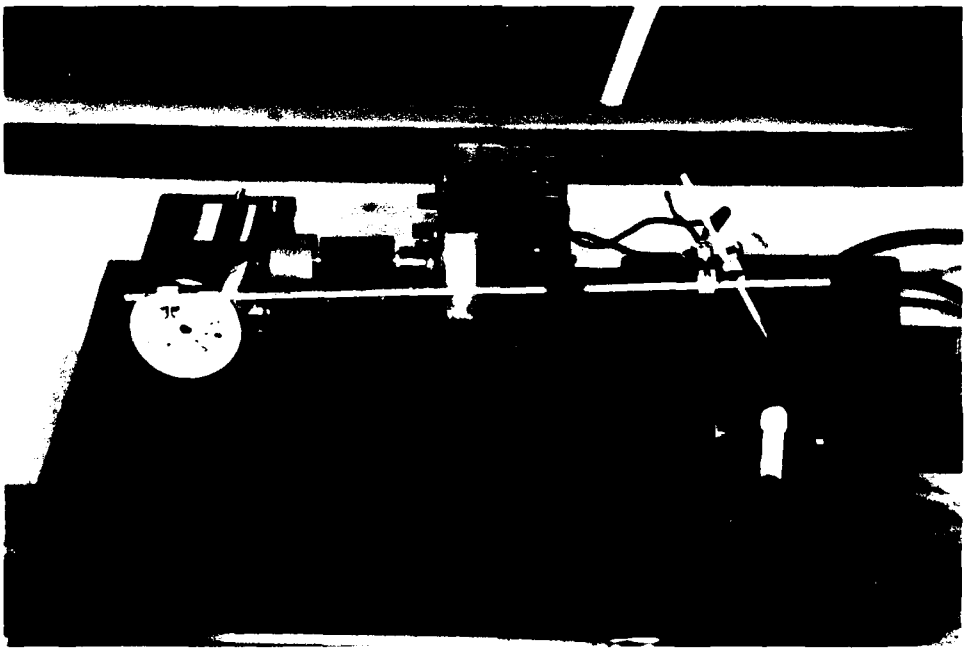

Fig. 8 - Forced-roll oscillation drive apparatus.

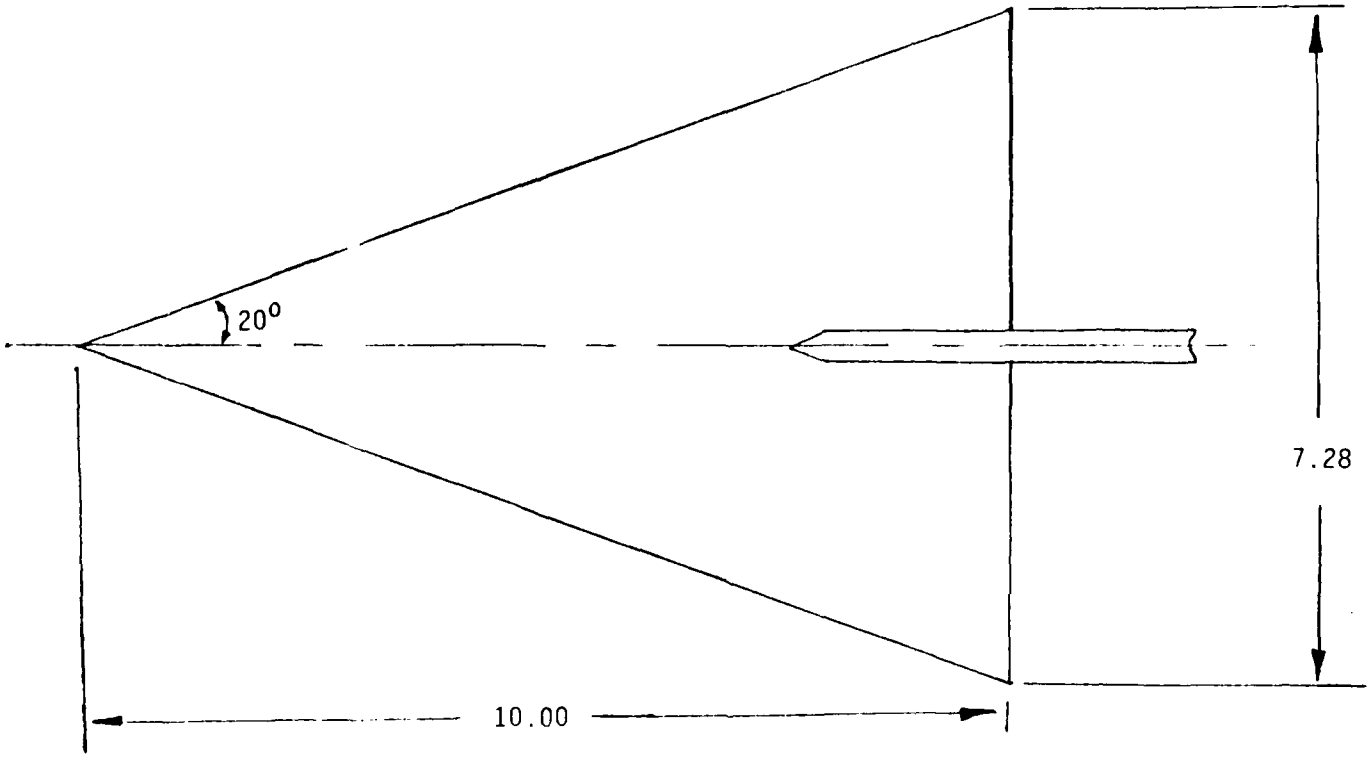

(a) 70° sweep

dimensions in inches

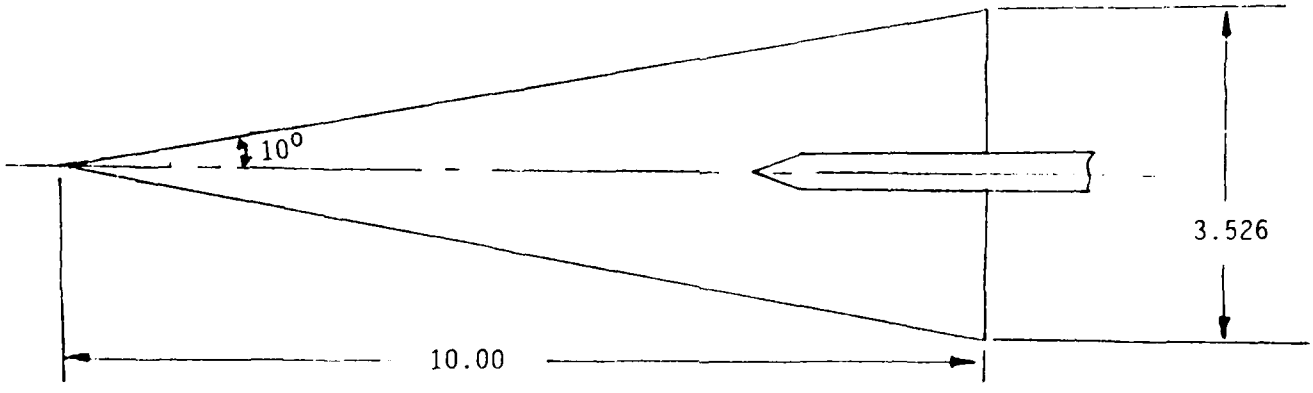

(b) 80° sweep

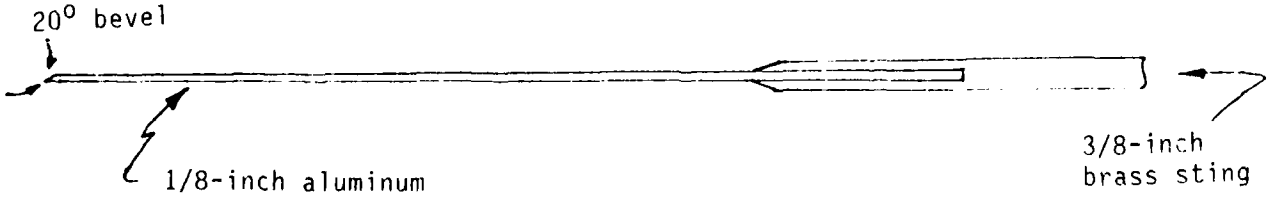

Fig. 9 - Delta wing water tunnel models.

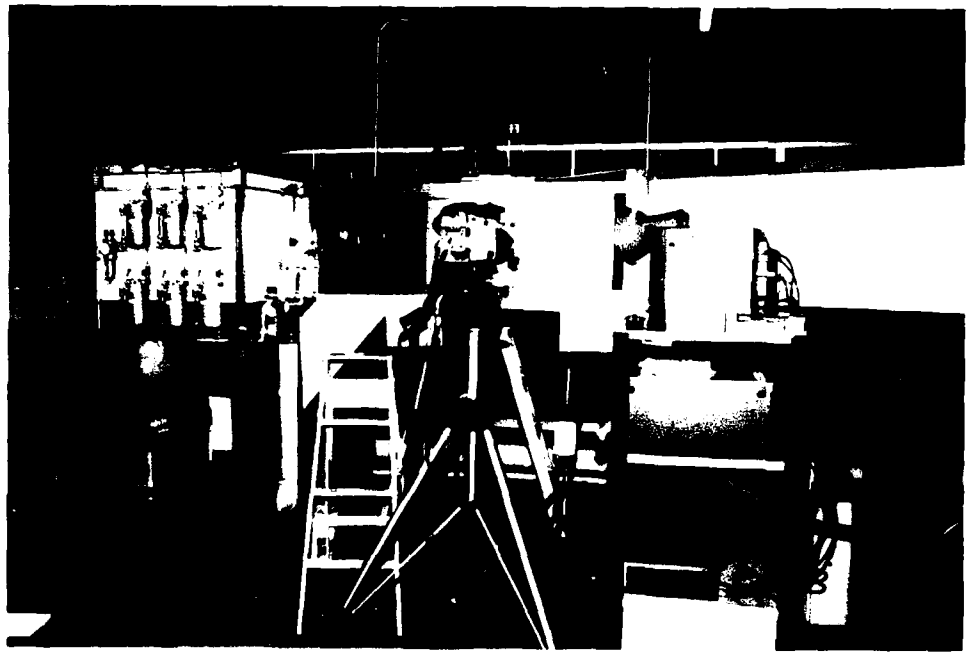

(a) Water tunnel, video cameras, monitors, and video processing equipment.

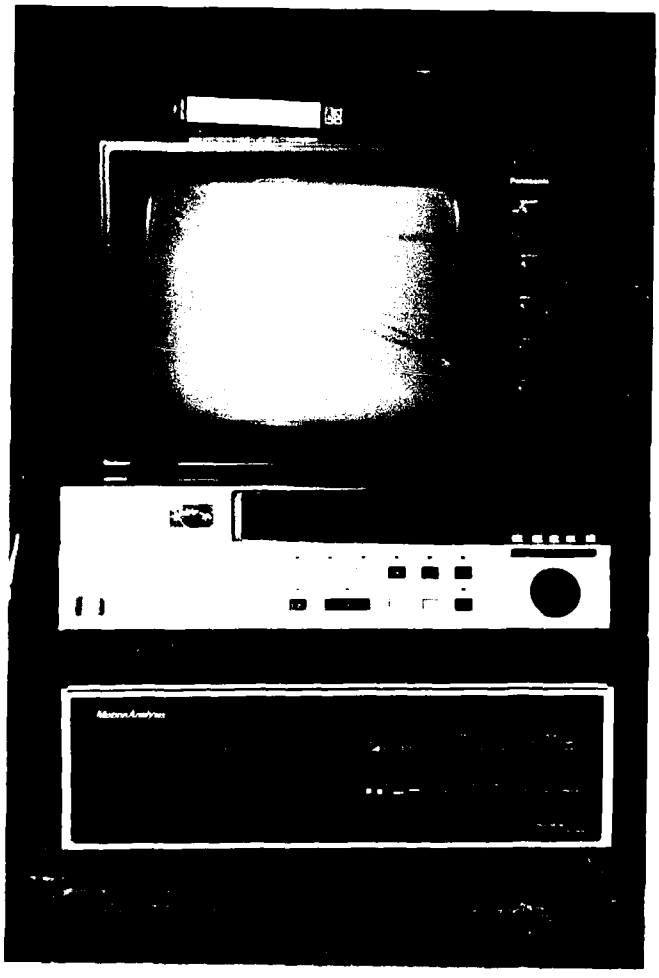

High Resolution Monitor

Playback VCR

ExpertVision Video Processor

(b) Video processor, VCR and monitor.

Fig. 11 - Water tunnel and video equipment required for ExpertVision system.

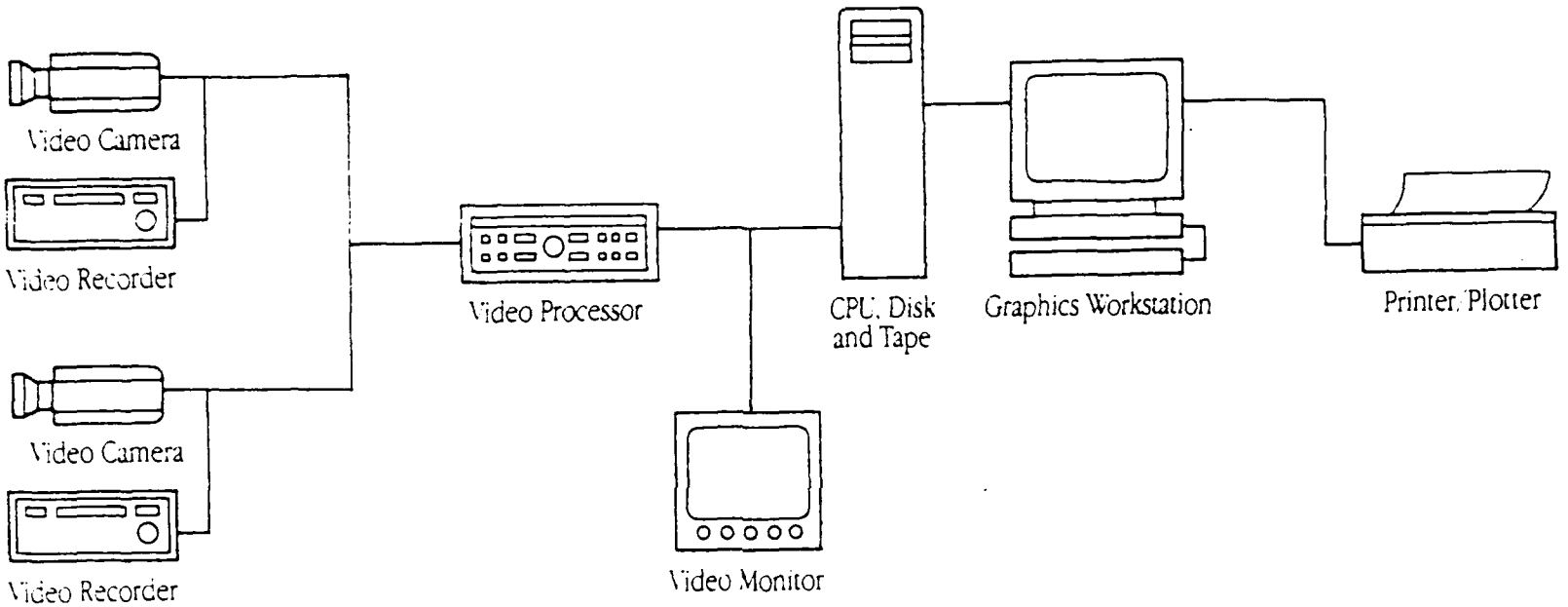

Fig. 10 - ExpertVision system components for 2-D flow measurements.

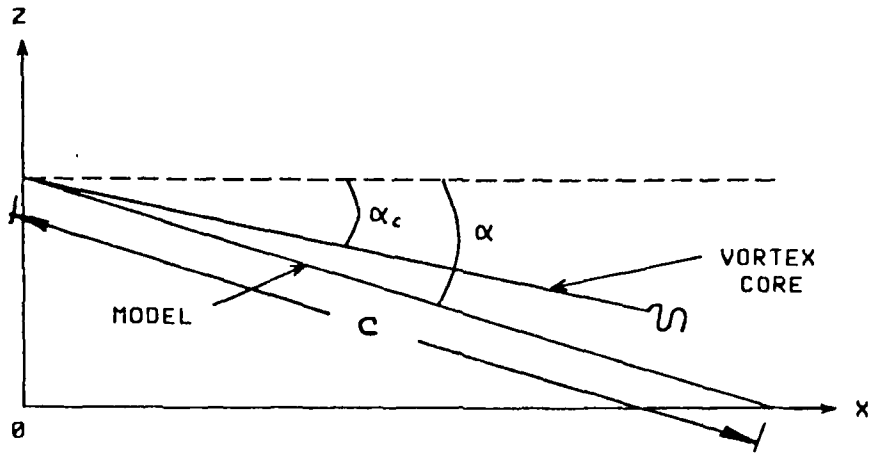

(a) Side view

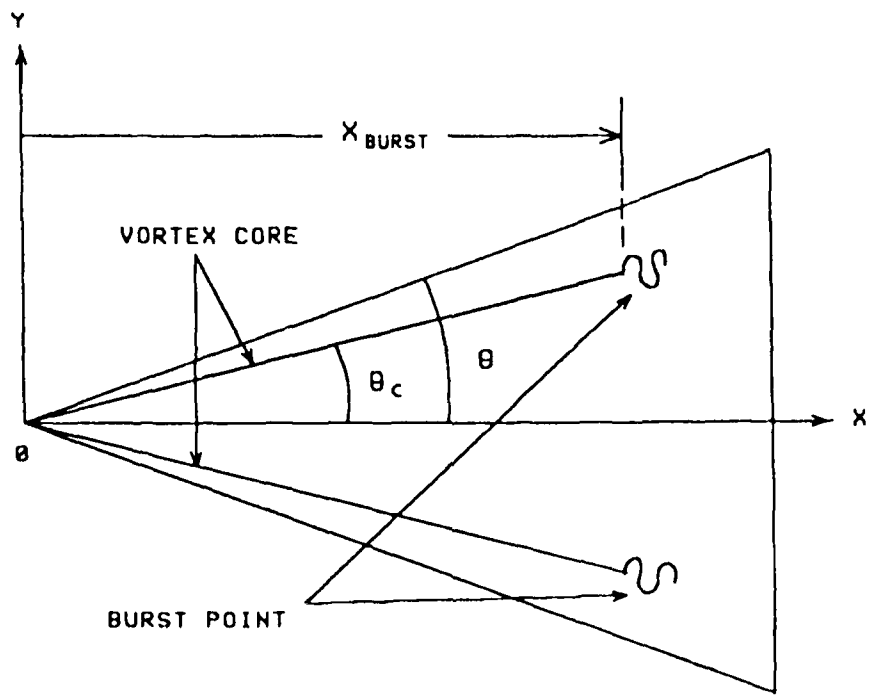

(b) Planform view

Fig. 12 - Vortex location parameters.

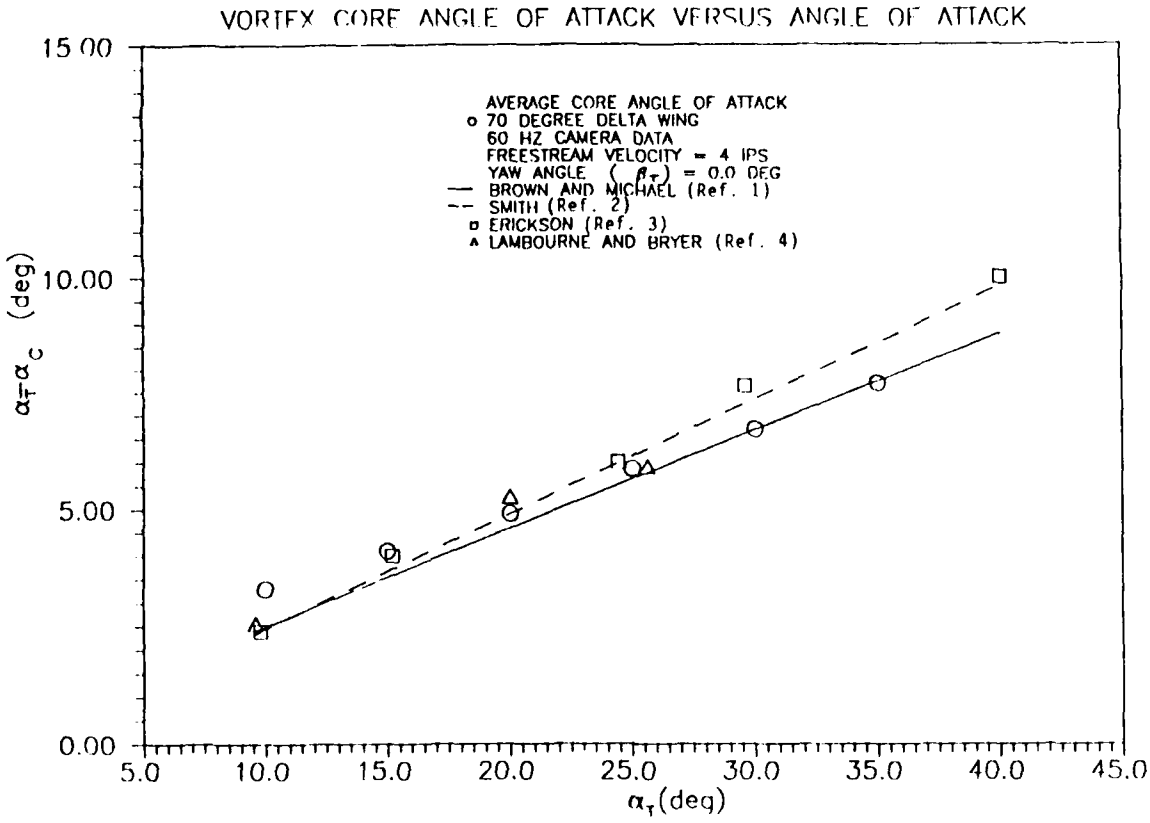

(a) Side view

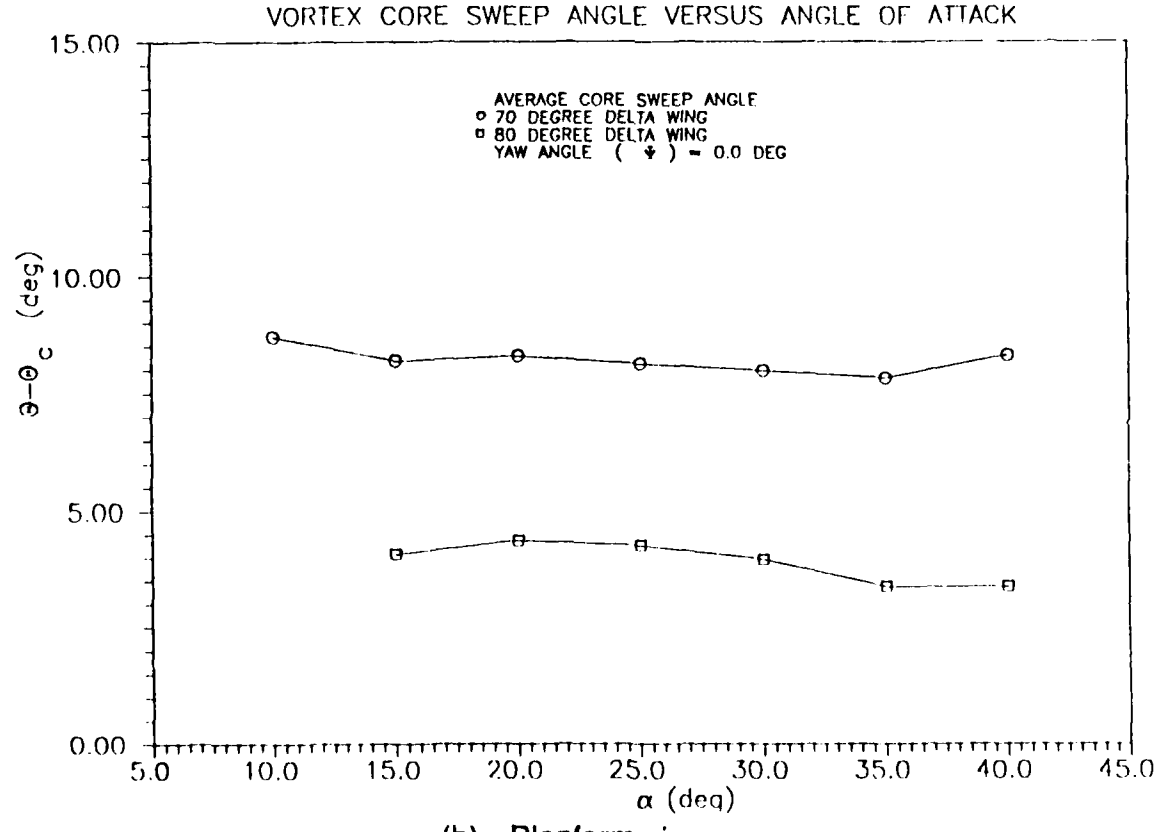

(b) Planform view

Fig. 13 - Vortex core locations.

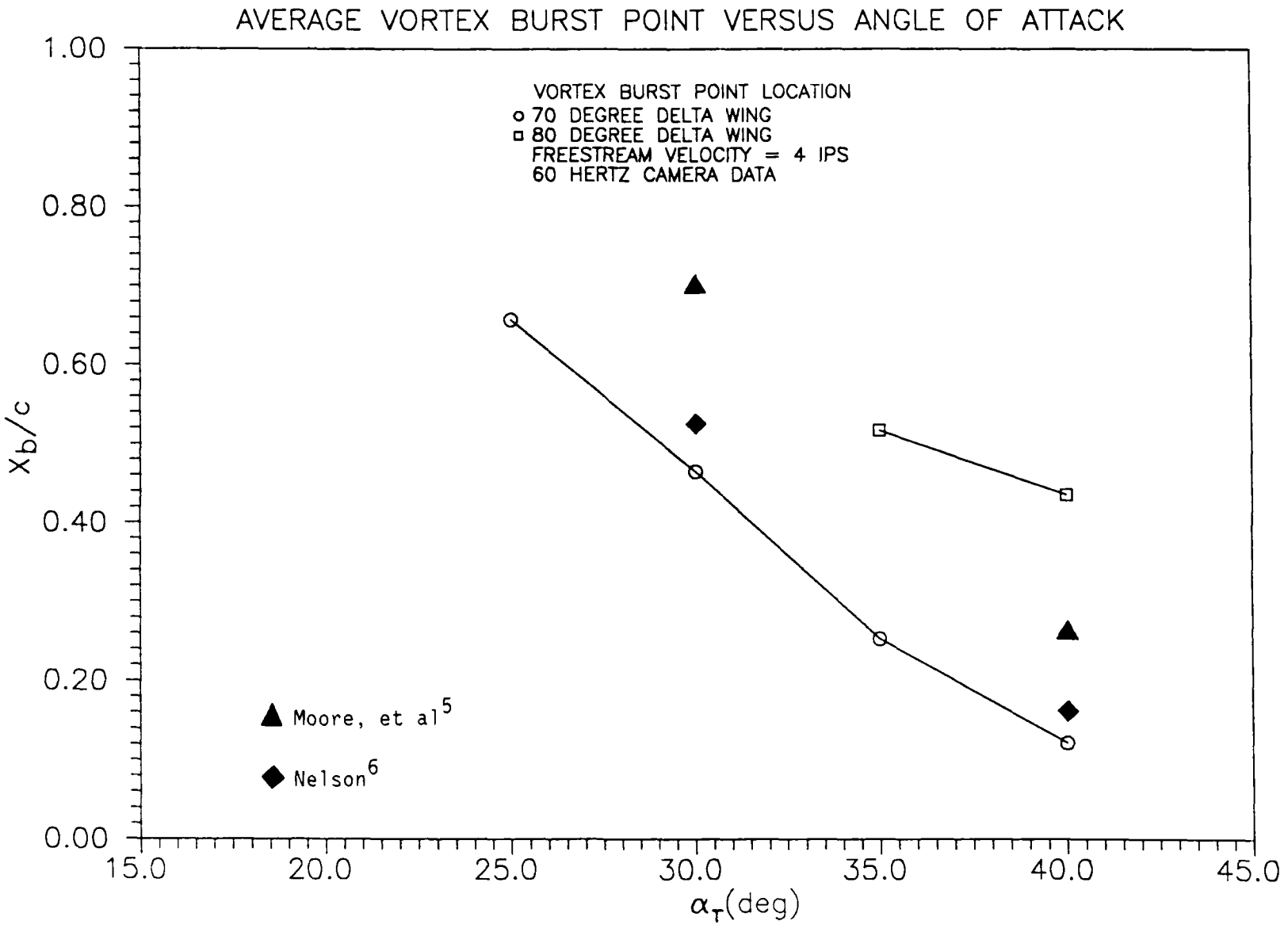

Fig. 14 - Average burst point locations for 70° and 80° wings at $\beta_T = 0$

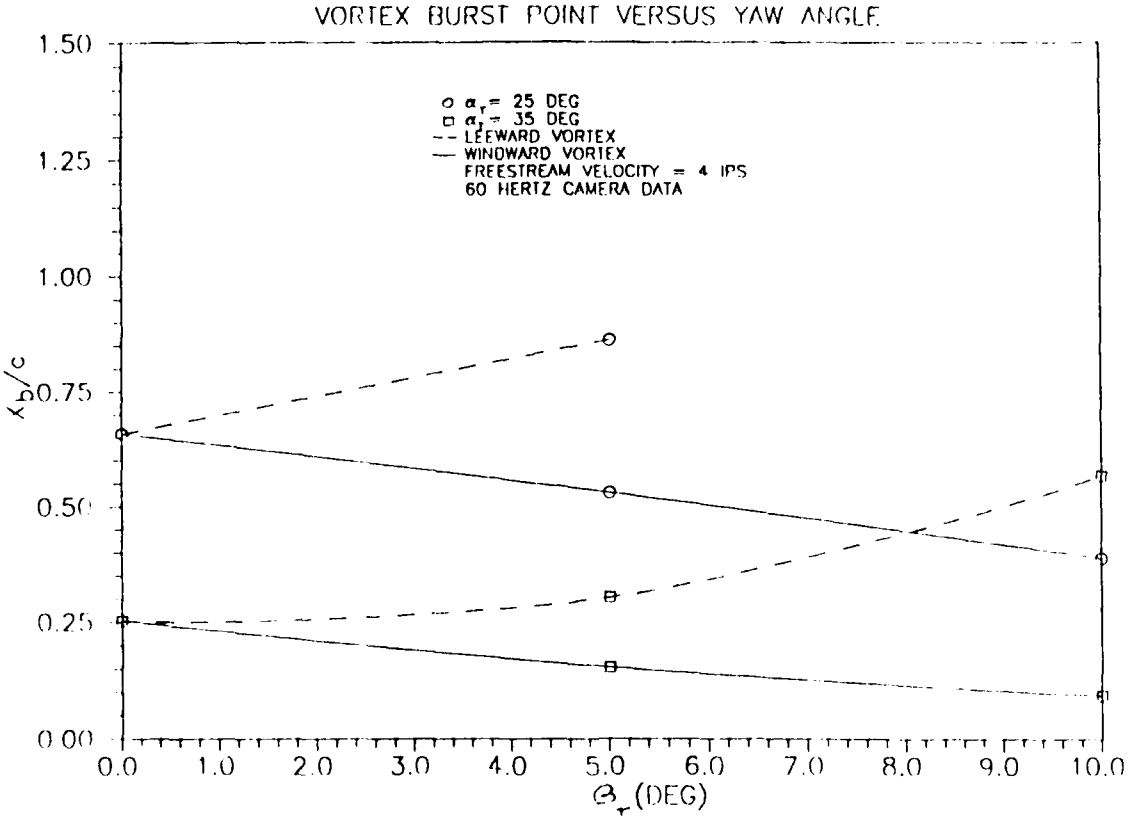

Fig. 15 - Average burst point locations vs yaw angle for 70° delta wing

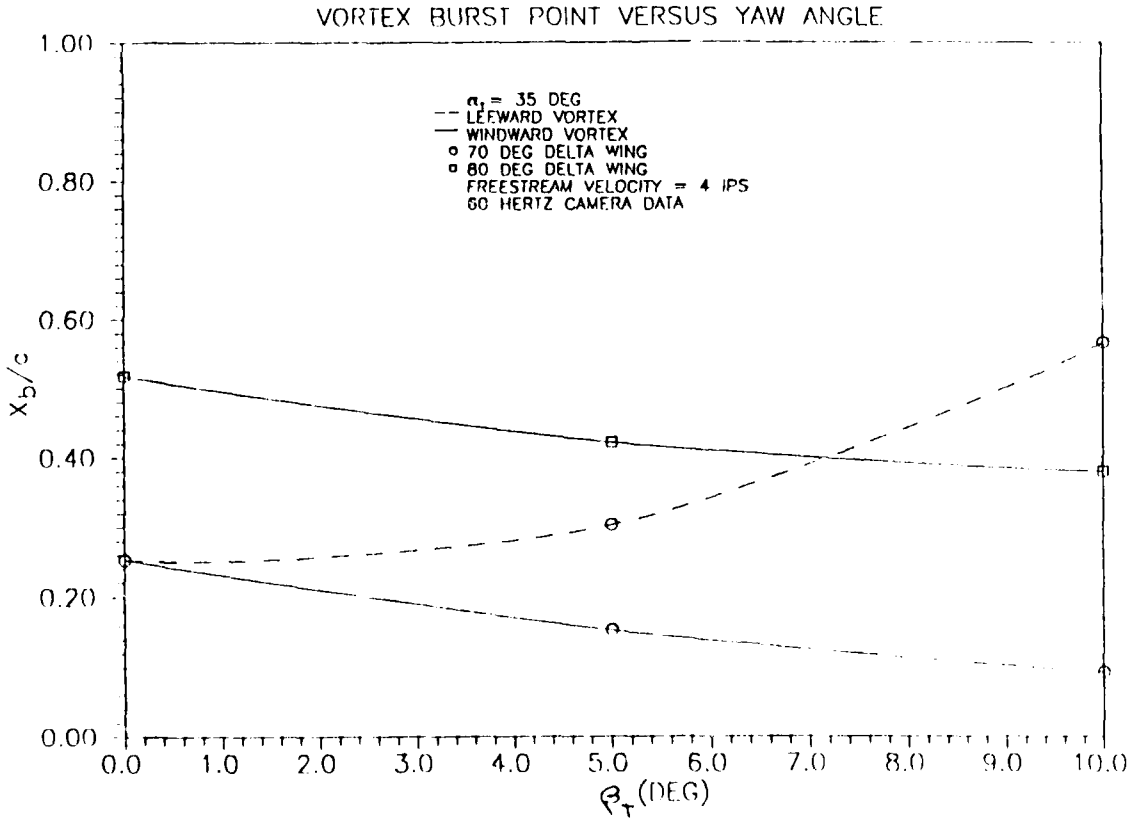

Fig. 16 - Average burst point locations vs yaw angle for 70° and 80° delta wings

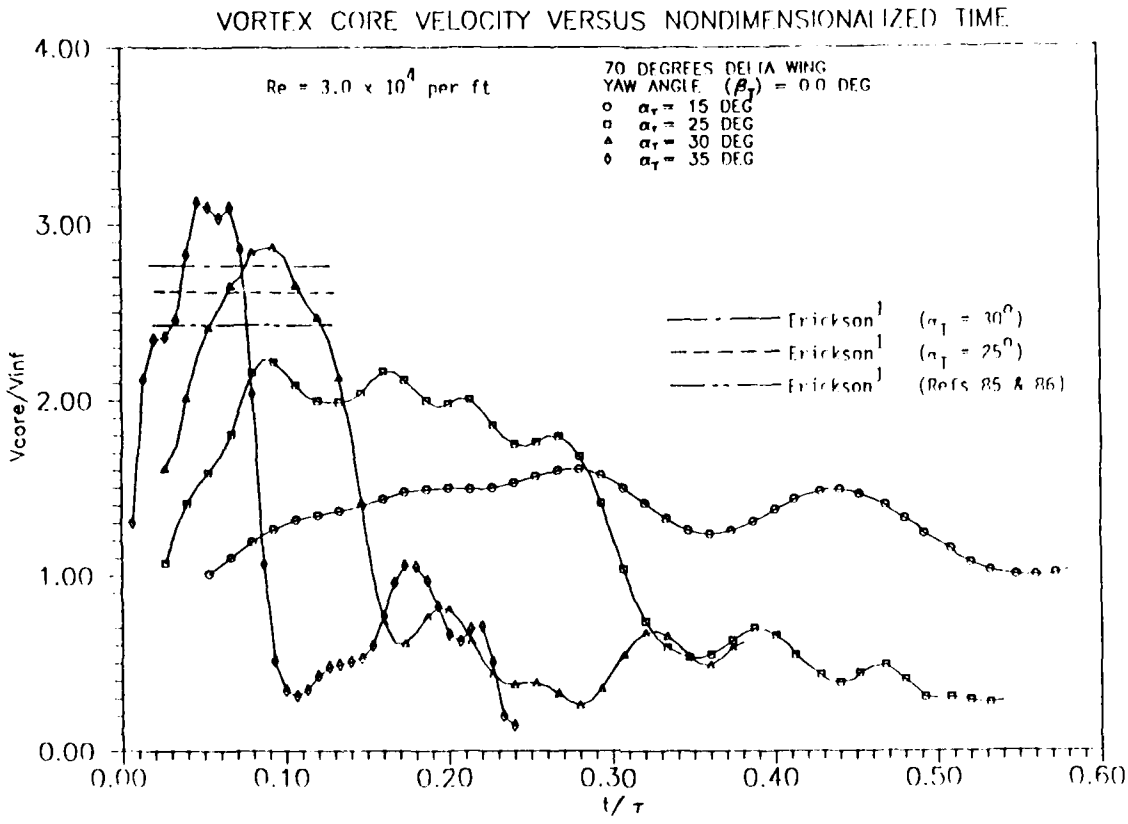

Fig. 17 - Nondimensional core velocities for 70° delta wing

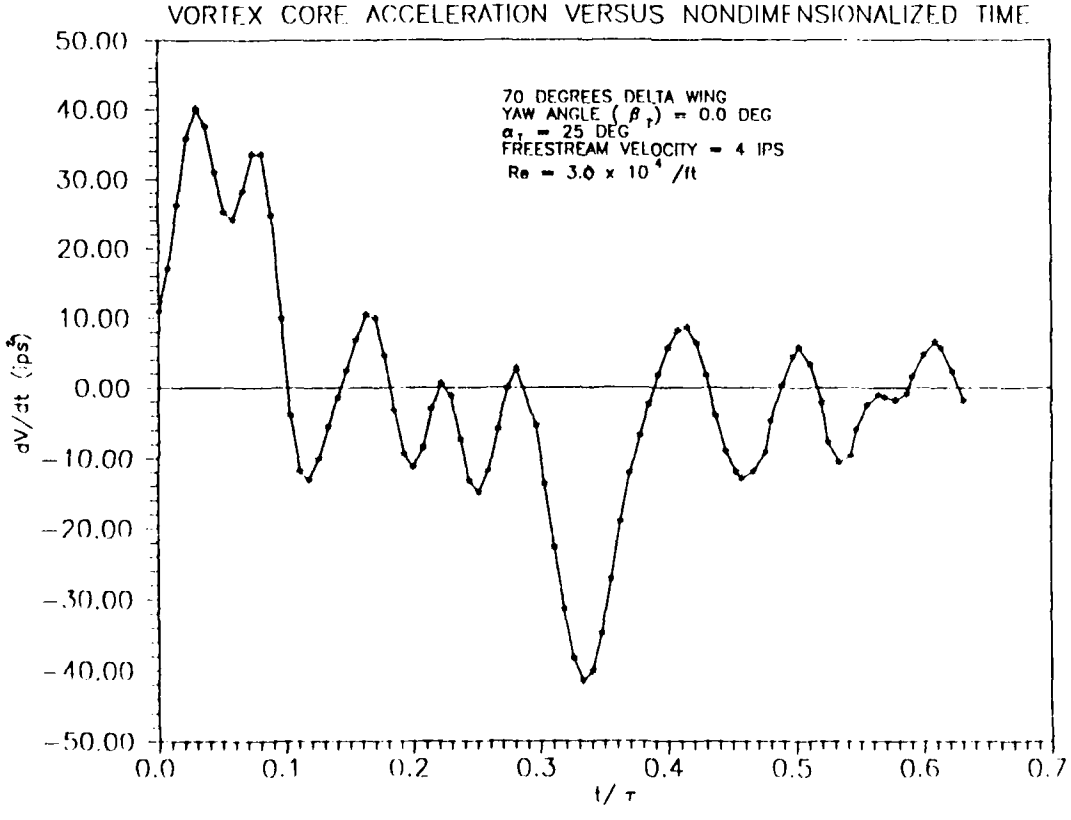

Fig. 18 Acceleration of a fluid element in the vortex core for 70° delta wing

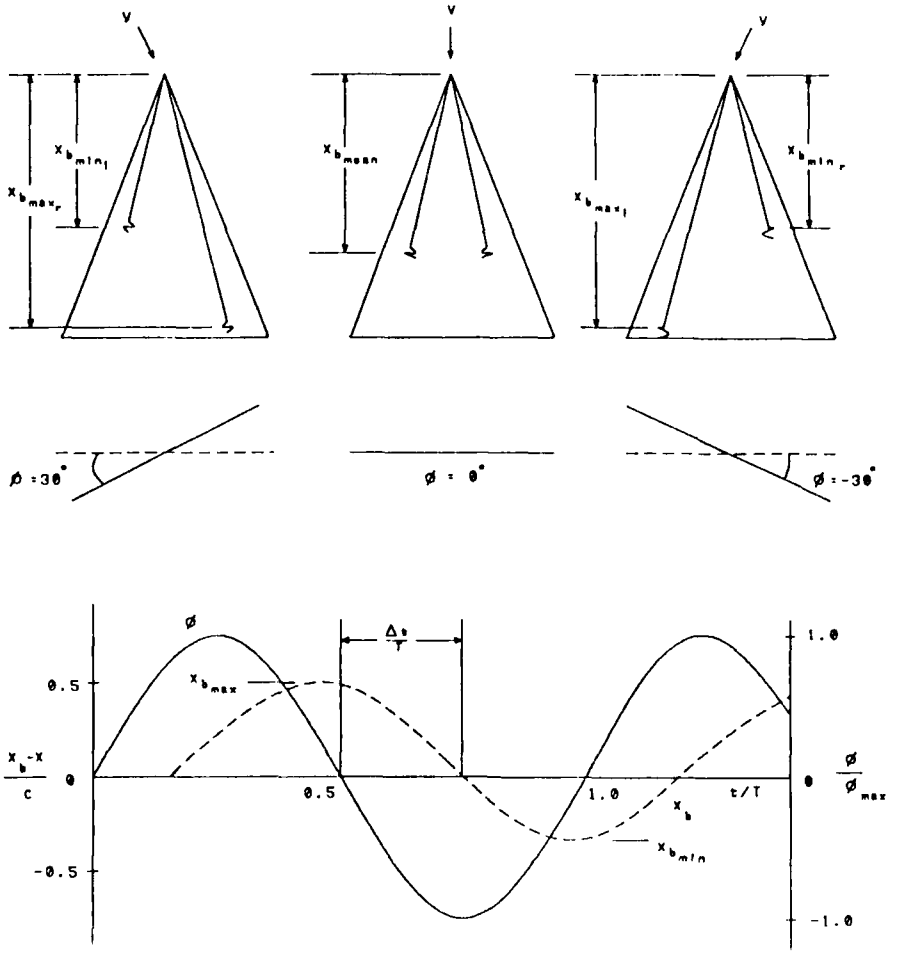

Fig. 19 - Definition of terms for oscillation-in-roll experiments

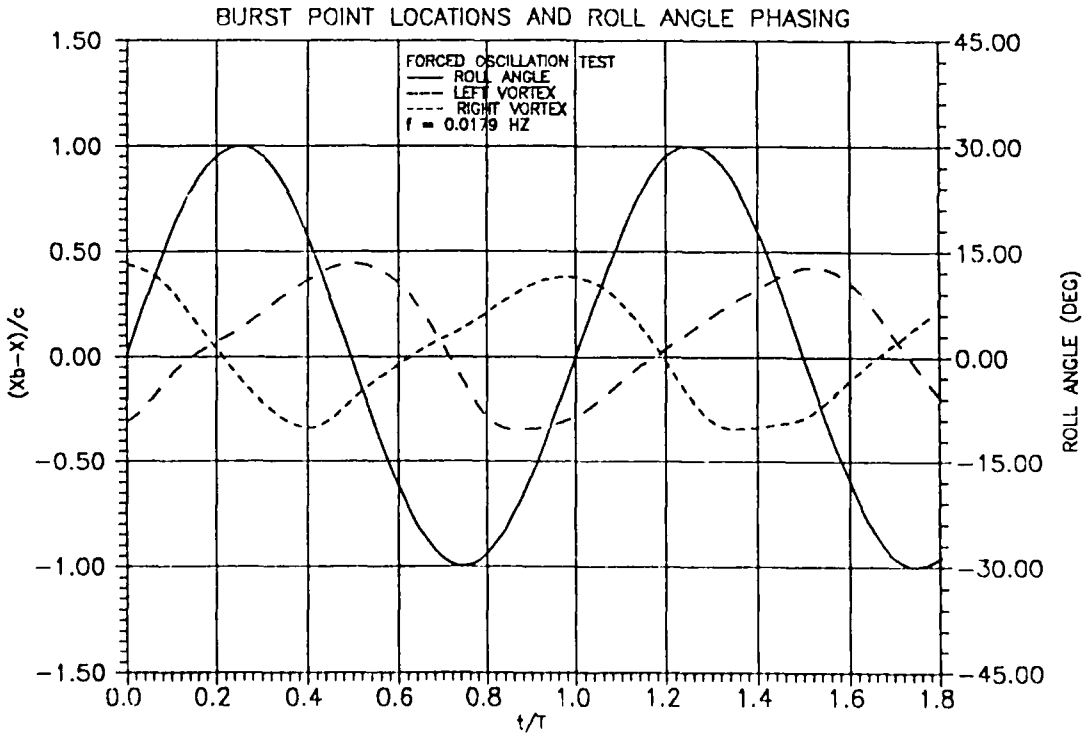

Fig. 20 - Burst point movement at f = 0.0179 (ω b/2v=0-.1) for 70° wing at α_T=25°

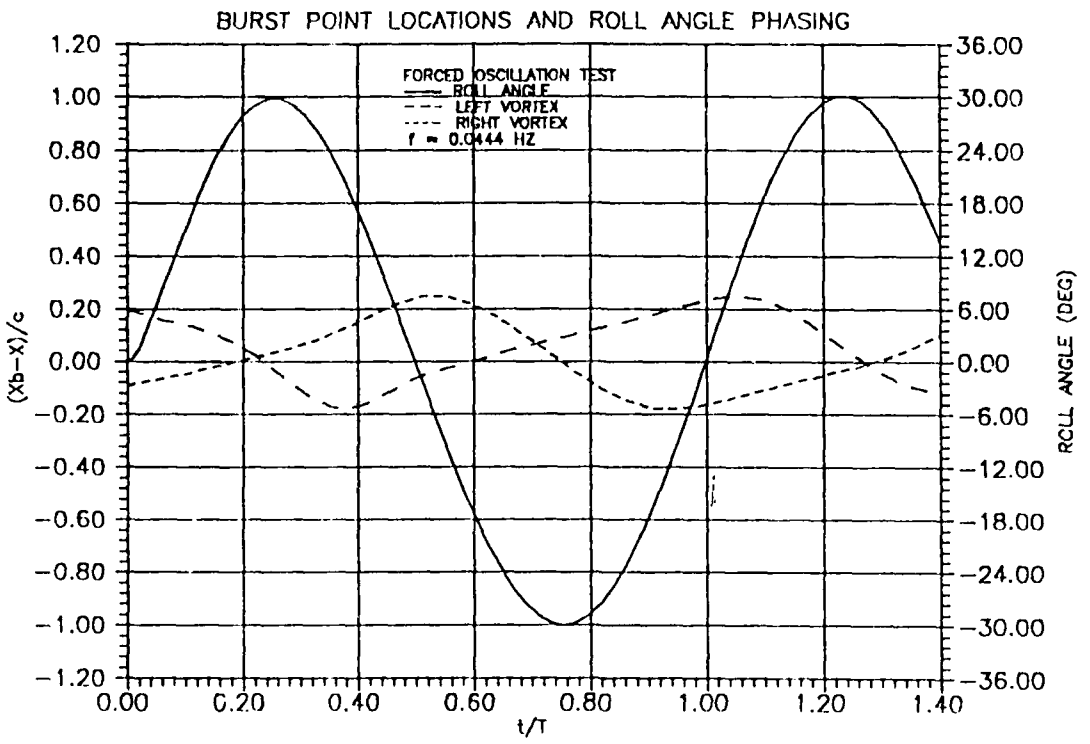

Fig. 21 · Burst point movement at f = 0.0444 (ω b/2v=0.25) for 70° wing at α_T=25°

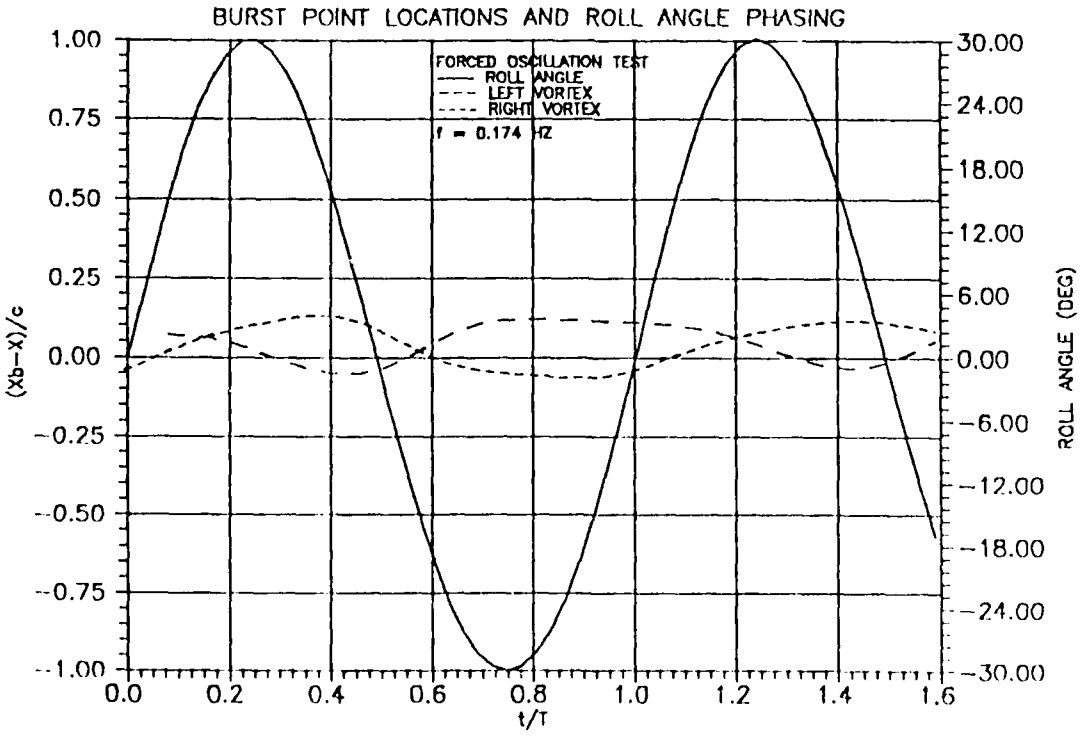

Fig. 22 Burst point movement at f = 0.174 (ω b/2v=1.0) for 70° wing at α_T=25°

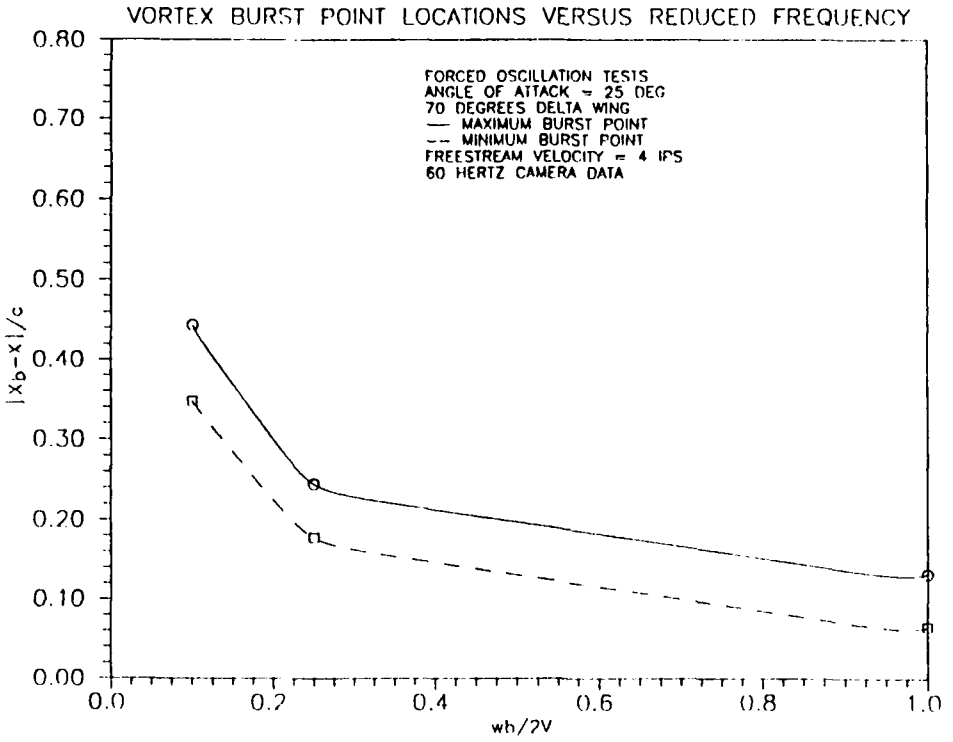

Fig. 23 - Variation of peak burst point location with roll oscillation frequency for 70° wing at α_T=25°

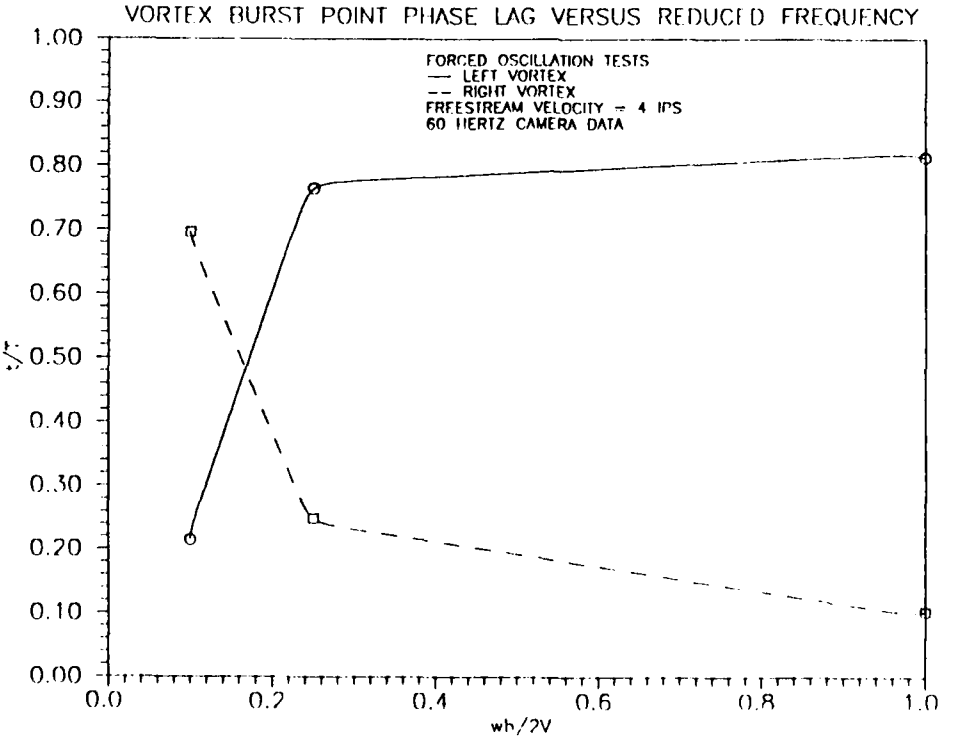

Fig. 24 - Phasing between burst point location and roll angle for 70° wing at α_T=25°

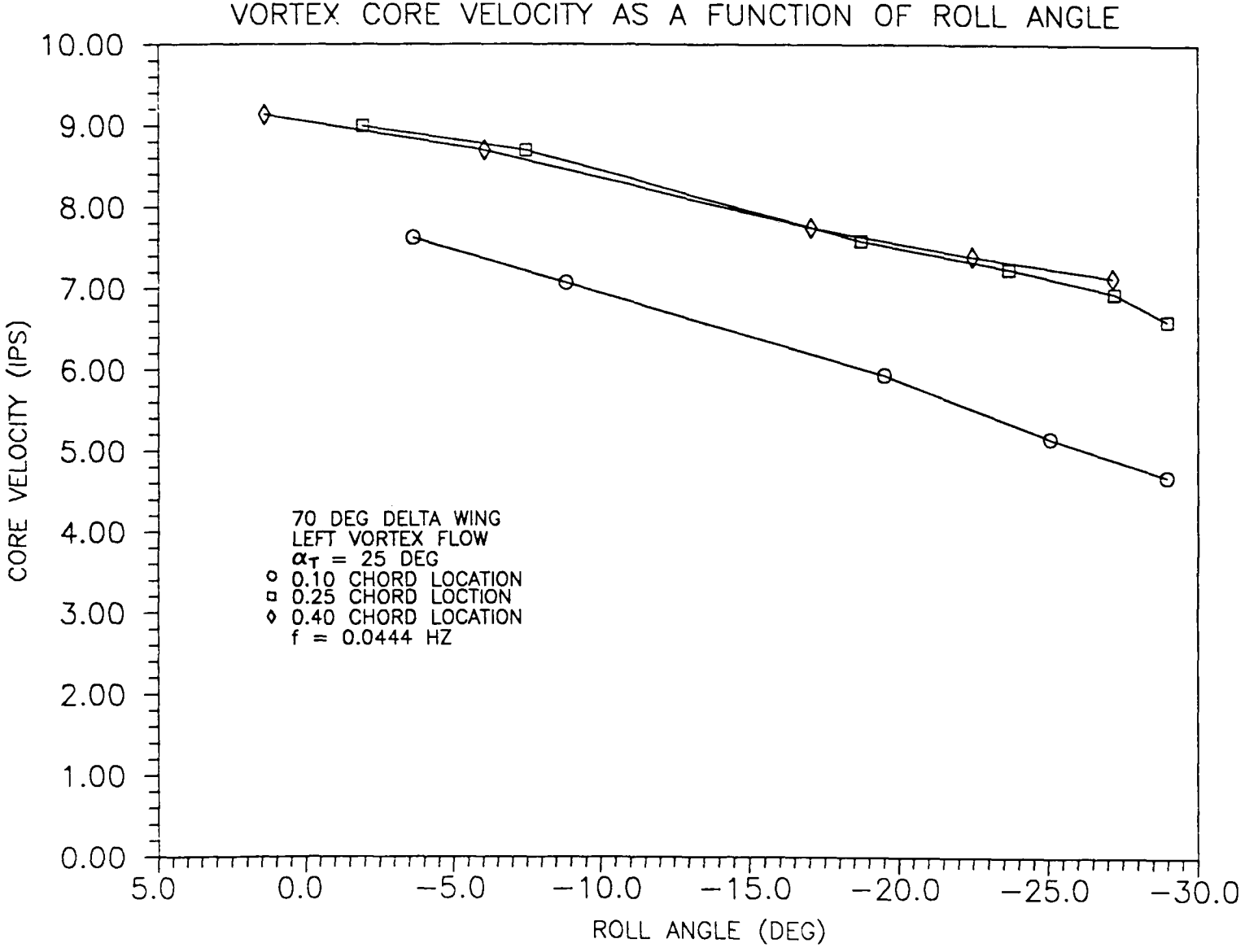

Fig. 25 - Left vortex core velocity vs model roll angle for 70° delta wing at α_T=25° and f=0.0444 Hz (ω b/2v=0.25)